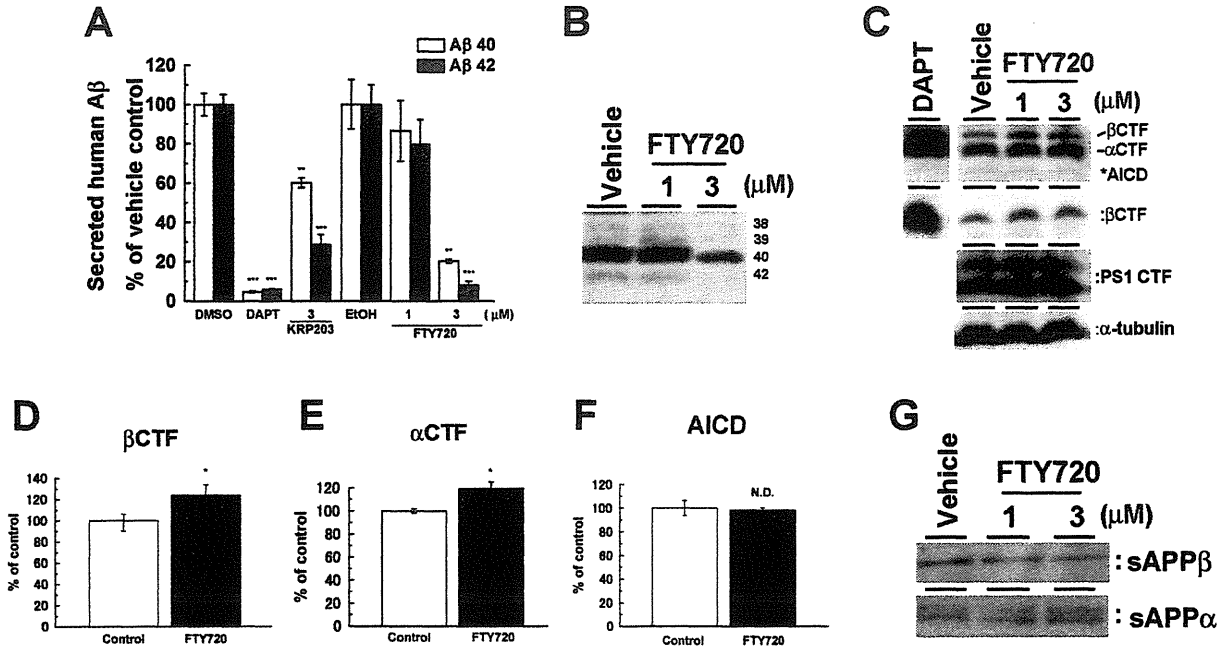

Figure 2. FTY720 decreased the γ-secretase-mediated cleavage of APP. SC100 were transiently transfected in N2a cells. After 24 hrs transfection, cells were treated with FTY720 or KRP203 for 24 hrs. (**A**) Levels of secreted human Aβ detected by human Aβ-specific ELISA (n = 4, mean ± SEM **P<0.01, ***P<0.001). (**B**) Immunoblotting analysis of secreted human Aβ separated by modified Tris/Tricin/8M Urea gel system. (**C**) Immunoblot analysis of APP CTFs including overexpressed SC100 and endogenous PS1 in FTY720-treated cell lysates. Quantification analysis of (**C**) for βCTF (**D**), αCTF (**E**) and AICD (**F**) (n = 4, mean ± SEM *P<0.05). (**G**) Immunoblot analysis of endogenous sAPPα and sAPPβ in the conditioned media of N2a cells.
doi:10.1371/journal.pone.0064050.g002

In vivo effects of FTY720 on Aβ levels in brains of AD model mice

FTY720 is known to cross the blood brain barrier and be accumulated in brains to suppress the inflammatory response in model mice of MS [19]. These data prompted us to test the *in vivo* effects of FTY720 in AD model mice. We subcutaneously injected FTY720 (0.5 mg/kg/day) for 6 days into 6-month-old female A7 transgenic mice overexpressing human APP carrying Swedish and Austrian double mutations [37]. At 6 months, A7 mice do not show amyloid plaques, whereas the levels of soluble Aβ are moderately increased compared to those in younger animals. Unexpectedly, we found that the level of soluble Aβ40 was decreased, whereas that of Aβ42 was significantly increased by a 6-days treatment with FTY720. This suggests that FTY720 treatment impacts on brain Aβ levels *in vivo*, although with some difference to its cellular effects.

Discussion

In this study, we examined the effect of S1PR modulators, FTY720 and KRP203, on brain Aβ and showed these compounds decreased Aβ production in neuronal cells. S1PR modulators decreased Aβ production also from βCTF, an APP-derived direct substrate of γ-secretase, without affecting AICD production nor the cleavage of Notch, suggesting that these reagents inhibited the carboxypeptidase-like γ-secretase activity. Sphk2 activity was required for the FTY720-mediated decrease of Aβ production, whereas the signaling cascade downstream of S1PR was dispensable for the effects of the FTY720. FTY720 was active also *in vivo* and decreased the levels of Aβ40 but increased those of Aβ42 in brains of APP transgenic mice. These results shed light on the complex regulatory function of S1PR modulators on brain Aβ.

Phosphorylation of FTY720 or KRP203 by SphK2 yields the active metabolite FTY720-P or KRP203-P, respectively, which acts as the ligand for S1PR1 [14,15,38]. It has been shown that phosphorylated S1PR modulators induce endocytosis of S1PR1 from the cell surface after binding to S1PR1, thereby causing the antagonistic effects [14,15]. Our RNAi suppression and overexpression studies showed that the SphK2 level was correlated to the capacity of FTY720 to decrease Aβ production (Fig. 3), supporting the view that phosphorylated forms of S1PR modulators are the *bona fide* active species that lower Aβ production. However, neither an authentic S1PR1 receptor an agonist SEW2871 nor antagonist W123 altered the Aβ production (Fig. S3). Moreover, co-treatment with W123 [41] or suramin [42] failed to cancel the inhibitory effect of FTY720 (Fig. 4), raising the possibility that the unconventional GPCR cascade is involved in the modulation of Aβ production. Interestingly, it has been shown that β2 adrenergic receptor [43] and an orphan G-protein receptor GPR3, the latter exhibiting a significant homology to S1PRs [44], affect the γ-secretase activity through the β-arrestin pathway [45,46,47]. β-Arrestins redistributes the γ-secretase complex toward detergent-resistant membranes, thereby increasing the catalytic activity of the complex [45,47]. This raises the possibility that S1PR modulators also alter the distribution of γ-secretase to regulate the APP-specific processing to generate Aβ. Another possibility would be that FTY720-P directly binds to γ-secretase or APP. FTY720 is known to accumulate within endosomes [48], in which mature γ-secretase and APP reside [10]. Interestingly, it has been shown that phosphatidylinositol 4,5-diphosphate (PI(4,5)P2), a

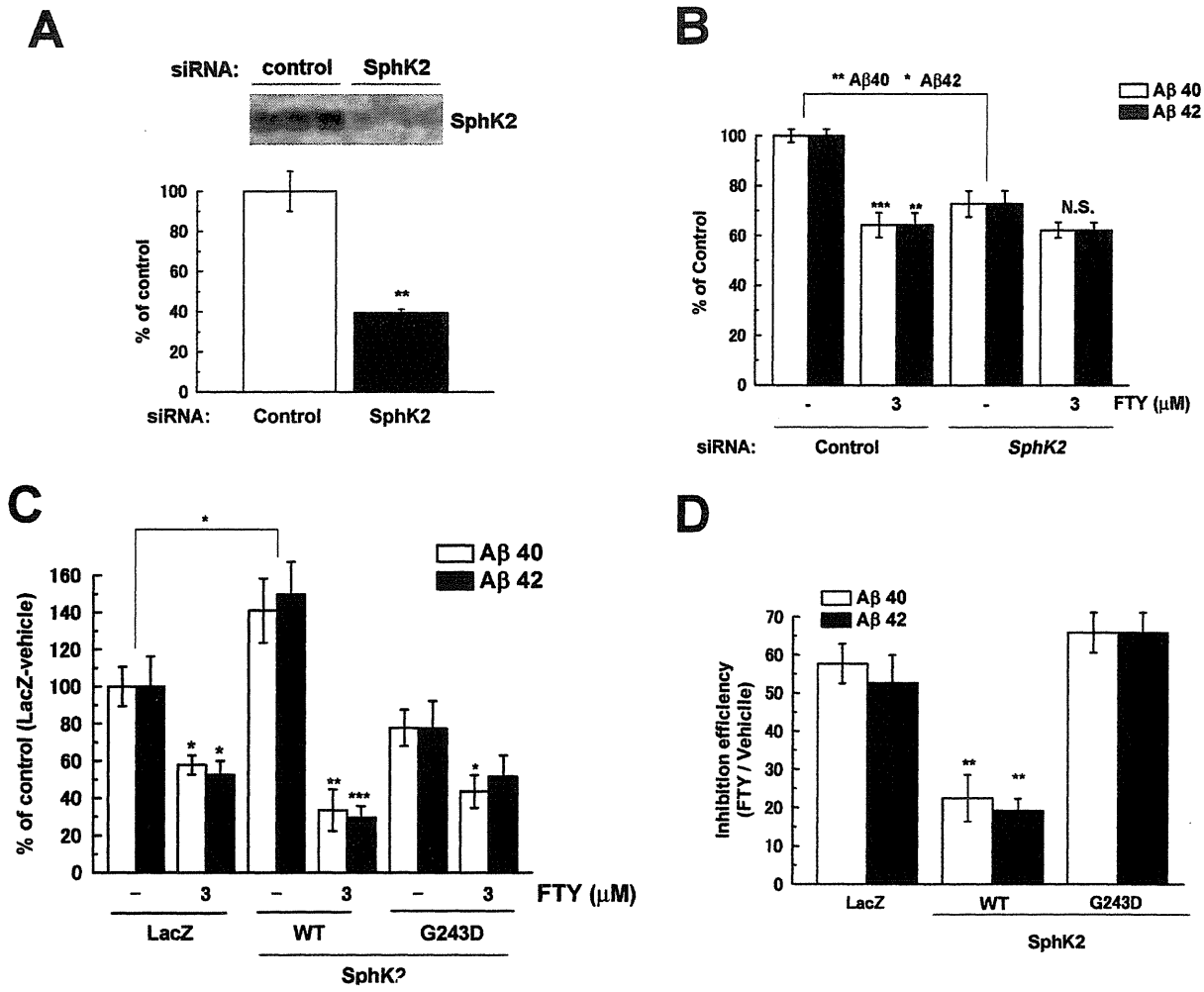

Figure 3. SphK2 activity is required for FTY720 mediated decrease of Aβ secretion. (**A**) N2a cells were transfected with siRNA against murine *SphK2*. After 48 hrs transfection of siRNA, levels of SphK2 was detected by immunoblotting (upper panel) and quantified (lower graph n = 3, mean ± SEM). (**B**) After 48 hrs transfection of siRNA, cells were treated with FTY720 for 24 hrs. Levels of secreted Aβ were quantified by ELISA (n = 3, mean ± SEM; *P<0.05, **P<0.01, ***P<0.001 compared with DMSO treatment or siRNA against *SphK2* (indicated by line)). One-way ANOVA with Tukey's post hoc test for individual treatment differences was used for statistical analysis. (**C, D**) N2a cells were transiently transfected with LacZ, wild-type (WT) or dominant negative mutant (G243D) SphK2. After 24 hrs transfection, cells were treated with FTY720 for 24 hrs. (**C**) Levels of secreted Aβ (n = 4, mean ± SEM; *P<0.05, **P<0.01, ***P<0.001 compared with DMSO treatment or SphK2 (indicated by line)). (**D**) The inhibitory efficiency of FTY720 on Aβ secretion compared with DMSO treatment in each transfection of (**C**). Secreted Aβ levels of FTY720 were standardized by vehicle control in each group (mean ± SEM; **P<0.01).
doi:10.1371/journal.pone.0064050.g003

representative phospholipid with a second messenger activity, directly binds to γ-secretase and inhibits its activity [49]. However, we observed extracellularly treated FTY720-P did not significantly alter the Aβ production. It would be important to note that controlled phosphorylation of S1PR modulators at appropriate intracellular locations is critical to their function [50]. Moreover, we are unable to rule out the possibility that other S1PRs or unknown receptor is involved in the FTY720-mediated γ-secretase inhibition. Further study is required to determine the precise intracellular site of phosphorylation, and distribution, of FTY720-P in specific membrane microdomains or organelles. The binding of FTY720-P to γ-secretase or APP should also be examined.

In contrast to the *in vitro* results in cells, a 6-days treatment of FTY720 decreased Aβ40, but increased Aβ42 in the brains of APP transgenic mice *in vivo* (Fig. 4D). We used a similar dosage of FTY720 that had been adopted in autoimmune model mice, which is expected to yield submicromolar levels of FTY720 in brains [19]. Thus, the unexpected rise in Aβ42 levels caused by FTY720 *in vivo* in brains might have been due to other mechanisms that are distinct from the modulation of the γ-secretase activity in cultured cells. Another possibility is that FTY720 affected the Aβ42 levels by negatively regulating the inflammatory responses in the central nervous system. FTY720 has been reported to inhibit the egress of T cell into the spinal cord in autoinflammatory response [19], as well as into the ischemic lesions in brain ischemia [51]. Interestingly, FTY720 also inhibited the migration of human monocytes induced by Aβ42 [52]. It is tempting to speculate that the FTY720 might have impacted on

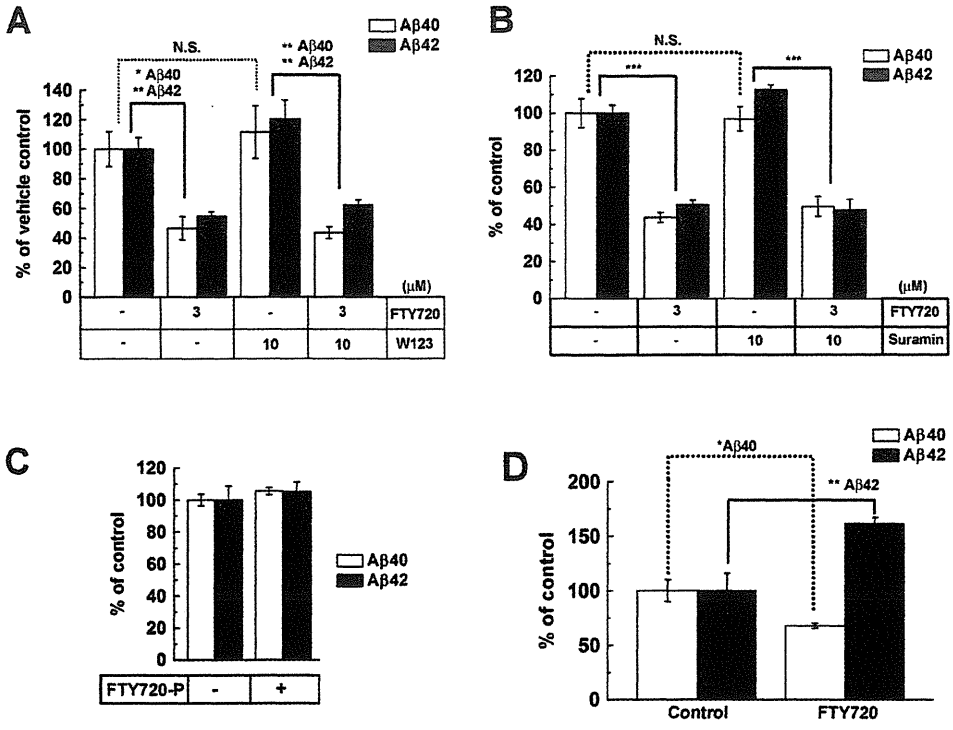

Figure 4. The effect of FTY720 on Aβ production is independent of downstream signaling of S1P receptors. (**A**) Levels of secreted Aβ from N2a cells co-treated with FTY720 and S1PR1 receptor antagonist W123 for 24 hrs (n = 4, mean ± SEM; *P<0.05, **P<0.01, N.S. no significant difference). (**B**) Levels of secreted Aβ from N2a cells co-treated with FTY720 and Gi protein inhibitor suramin for 24 hrs (n = 4, mean ± SEM; ***P<0.001, N.S. no significant difference). (**C**) Levels of secreted Aβ from N2a cells treated with FTY720-P for 24 hrs (n = 4, mean ± SEM). (**D**) *In vivo* effect of FTY720 on Aβ levels in AD model mice brain. Levels of soluble Aβ in the cerebral cortices of female A7 mice at 6 months of age after 6-days treatment with FTY720 (0.5 mg/kg/day, s.c.). Total brain human Aβ levels were measured by human-Aβ specific sandwich ELISA (n = 3–4, mean ± SEM, *P<0.05, ** p<0.01).
doi:10.1371/journal.pone.0064050.g004

the Aβ42 metabolism *in vivo* through altering the clearance of Aβ42 by microglial cells, overriding the inhibitory effects on neurons. As FTY720 has been approved for MS therapy in clinics, the regulatory mechanisms whereby S1PR modulators impact on Aβ42 metabolism, as well as on the inflammatory responses in AD brains, should further be characterized, in the light of therapeutics as well as adverse effects in humans. In sum, we identified a novel role of S1PR modulators on Aβ, which may open up a novel aspect in Aβ metabolism and lead to a novel therapeutic strategy for AD.

Supporting Information

Figure S1 AlamarBlue assay of N2aNH cells treated with S1PR modulators. After 24 hr treatment with S1PR modulators, N2aNH cells were incubated with cultured medium containing almarBlue (Invitrogen). Medium was collected to monitor fluorescence at 530–560/590 nm excitation/emission wavelengthes.
(TIF)

Figure S2 Effect of S1PR1 agonist and antagonist on ERK1/2 phosphorylation. Immunoblotting analysis of N2a cell lysates for ERK1/2 phosphorylation. Prior to stimulation with the indicated compounds, N2a cells were starved in serum free medium for 6 hr. Results of densitometric analysis of phosphorylated ERK1/2 (compared with control) are shown below the columns. (**A**) N2a cells were incubated for 10 min with the FTY720 (1 μM), FTY720-P (1 μM), SEW2871 (1 μM), and PKC activator PMA (Phorbol 12-Myristate 13-acetate; 1 μM), which in known as an activator of ERK1/2 phosphorylation. (**B**) N2a cells were preincubated with or without 1 μM W123 for 10 min. After addition of 1 μM SEW2871, cells were further incubated for 30 min and harvested for immunoblotting.
(TIF)

Figure S3 Dose dependent responses of S1PR1 agonist and antagonist on N2aNH cells. N2aNH cells were treated with SEW2871 or W123 for 24 hr at indicated doses. These reagents have no toxicity at 0.3, 1, 3, and 10 μM (**A**; alamarBlue assay), and failed to affect the Aβ40 production at indicated doses (**B**).
(TIF)

Acknowledgments

The authors are grateful to Drs. R. Kopan (Washington University in St. Louis) and J. Naslund (Karolinska Institutet in Sweden) for valuable reagents, Takeda pharmaceutical company for Aβ ELISA, and our current and previous laboratory members for helpful discussions and technical assistance.

Author Contributions

Conceived and designed the experiments: NT TT. Performed the experiments: NT TS IE SO HI. Analyzed the data: NT TT. Contributed reagents/materials/analysis tools: KT. Wrote the paper: NT TT TI.

References

1. Haughey NJ, Bandaru VV, Bae M, Mattson MP (2010) Roles for dysfunctional sphingolipid metabolism in Alzheimer's disease neuropathogenesis. Biochimica et biophysica acta 1801: 878–886.
2. Cutler RG, Kelly J, Storie K, Pedersen WA, Tammara A, et al. (2004) Involvement of oxidative stress-induced abnormalities in ceramide and cholesterol metabolism in brain aging and Alzheimer's disease. Proceedings of the National Academy of Sciences of the United States of America 101: 2070–2075.
3. Han X, D MH, McKeel DW, Jr., Kelley J, Morris JC (2002) Substantial sulfatide deficiency and ceramide elevation in very early Alzheimer's disease: potential role in disease pathogenesis. Journal of neurochemistry 82: 809–818.
4. He X, Huang Y, Li B, Gong CX, Schuchman EH (2010) Deregulation of sphingolipid metabolism in Alzheimer's disease. Neurobiology of aging 31: 398–408.
5. Grimm MO, Rothhaar TL, Hartmann T (2012) The role of APP proteolytic processing in lipid metabolism. Experimental brain research Experimentelle Hirnforschung Experimentation cerebrale 217: 365–375.
6. Tomita T (2009) Secretase inhibitors and modulators for Alzheimer's disease treatment. Expert review of neurotherapeutics 9: 661–679.
7. De Strooper B, Vassar R, Golde T (2010) The secretases: enzymes with therapeutic potential in Alzheimer disease. Nature reviews Neurology 6: 99–107.
8. Vassar R, Kovacs DM, Yan R, Wong PC (2009) The beta-secretase enzyme BACE in health and Alzheimer's disease: regulation, cell biology, function, and therapeutic potential. The Journal of neuroscience: the official journal of the Society for Neuroscience 29: 12787–12794.
9. Takasugi N, Tomita T, Hayashi I, Tsuruoka M, Niimura M, et al. (2003) The role of presenilin cofactors in the gamma-secretase complex. Nature 422: 438–441.
10. Vetrivel KS, Thinakaran G (2010) Membrane rafts in Alzheimer's disease beta-amyloid production. Biochimica et biophysica acta 1801: 860–867.
11. Kalvodova L, Kahya N, Schwille P, Ehehalt R, Verkade P, et al. (2005) Lipids as modulators of proteolytic activity of BACE: involvement of cholesterol, glycosphingolipids, and anionic phospholipids in vitro. The Journal of biological chemistry 280: 36815–36823.
12. Osenkowski P, Ye W, Wang R, Wolfe MS, Selkoe DJ (2008) Direct and potent regulation of gamma-secretase by its lipid microenvironment. The Journal of biological chemistry 283: 22529–22540.
13. Holmes O, Paturi S, Ye W, Wolfe MS, Selkoe DJ (2012) Effects of membrane lipids on the activity and processivity of purified gamma-secretase. Biochemistry 51: 3565–3575.
14. Brinkmann V, Billich A, Baumruker T, Heining P, Schmouder R, et al. (2010) Fingolimod (FTY720): discovery and development of an oral drug to treat multiple sclerosis. Nat Rev Drug Discov 9: 883–897.
15. Aktas O, Kury P, Kieseier B, Hartung HP (2010) Fingolimod is a potential novel therapy for multiple sclerosis. Nat Rev Neurol 6: 373–382.
16. Zemann B, Kinzel B, Muller M, Reuschel R, Mechtcheriakova D, et al. (2006) Sphingosine kinase type 2 is essential for lymphopenia induced by the immunomodulatory drug FTY720. Blood 107: 1454–1458.
17. Don AS, Martinez-Lamenca C, Webb WR, Proia RL, Roberts E, et al. (2007) Essential requirement for sphingosine kinase 2 in a sphingolipid apoptosis pathway activated by FTY720 analogues. J Biol Chem 282: 15833–15842.
18. Hogenauer K, Billich A, Pally C, Streiff M, Wagner T, et al. (2008) Phosphorylation by sphingosine kinase 2 is essential for in vivo potency of FTY720 analogues. ChemMedChem 3: 1027–1029.
19. Foster CA, Howard LM, Schweitzer A, Persohn E, Hiestand PC, et al. (2007) Brain penetration of the oral immunomodulatory drug FTY720 and its phosphorylation in the central nervous system during experimental autoimmune encephalomyelitis: consequences for mode of action in multiple sclerosis. J Pharmacol Exp Ther 323: 469–475.
20. Choi JW, Gardell SE, Herr DR, Rivera R, Lee CW, et al. (2011) FTY720 (fingolimod) efficacy in an animal model of multiple sclerosis requires astrocyte sphingosine 1-phosphate receptor 1 (S1P1) modulation. Proceedings of the National Academy of Sciences of the United States of America 108: 751–756.
21. Fujino M, Funeshima N, Kitazawa Y, Kimura H, Amemiya H, et al. (2003) Amelioration of experimental autoimmune encephalomyelitis in Lewis rats by FTY720 treatment. The Journal of pharmacology and experimental therapeutics 305: 70–77.
22. Takasugi N, Sasaki T, Suzuki K, Osawa S, Isshiki H, et al. (2011) BACE1 Activity Is Modulated by Cell-Associated Sphingosine-1-Phosphate. The Journal of neuroscience: the official journal of the Society for Neuroscience 31: 6850–6857.
23. Kaneko T, Murakami T, Kawana H, Takahashi M, Yasue T, et al. (2006) Sphingosine-1-phosphate receptor agonists suppress concanavalin A-induced hepatic injury in mice. Biochemical and biophysical research communications 345: 85–92.
24. Kan T, Tominari Y, Morohashi Y, Natsugari H, Tomita T, et al. (2003) Solid-phase synthesis of photoaffinity probes: highly efficient incorporation of biotin-tag and cross-linking groups. Chemical communications: 2244–2245.
25. Tomita T, Takikawa R, Koyama A, Morohashi Y, Takasugi N, et al. (1999) C terminus of presenilin is required for overproduction of amyloidogenic Abeta42 through stabilization and endoproteolysis of presenilin. The Journal of neuroscience: the official journal of the Society for Neuroscience 19: 10627–10634.
26. Tomita T, Maruyama K, Saido TC, Kume H, Shinozaki K, et al. (1997) The presenilin 2 mutation (N141I) linked to familial Alzheimer disease (Volga German families) increases the secretion of amyloid beta protein ending at the 42nd (or 43rd) residue. Proceedings of the National Academy of Sciences of the United States of America 94: 2025–2030.
27. Iwatsubo T, Odaka A, Suzuki N, Mizusawa H, Nukina N, et al. (1994) Visualization of A beta 42(43) and A beta 40 in senile plaques with end-specific A beta monoclonals: evidence that an initially deposited species is A beta 42(43). Neuron 13: 45–53.
28. Qi-Takahara Y, Morishima-Kawashima M, Tanimura Y, Dolios G, Hirotani N, et al. (2005) Longer forms of amyloid beta protein: implications for the mechanism of intramembrane cleavage by gamma-secretase. The Journal of neuroscience: the official journal of the Society for Neuroscience 25: 436–445.
29. Merhi A, Andre B (2012) Internal amino acids promote Gap1 permease ubiquitylation via TORC1/Npr1/14-3-3-dependent control of the Bul arrestin-like adaptors. Mol Cell Biol 32: 4510–4522.
30. Kopan R, Schroeter EH, Weintraub H, Nye JS (1996) Signal transduction by activated mNotch: importance of proteolytic processing and its regulation by the extracellular domain. Proceedings of the National Academy of Sciences of the United States of America 93: 1683–1688.
31. Iwata H, Tomita T, Maruyama K, Iwatsubo T (2001) Subcellular compartment and molecular subdomain of beta-amyloid precursor protein relevant to the Abeta 42-promoting effects of Alzheimer mutant presenilin 2. The Journal of biological chemistry 276: 21678–21685.
32. Imamura Y, Watanabe N, Umezawa N, Iwatsubo T, Kato N, et al. (2009) Inhibition of gamma-secretase activity by helical beta-peptide foldamers. Journal of the American Chemical Society 131: 7353–7359.
33. Becuwe M, Herrador A, Haguenauer-Tsapis R, Vincent O, Leon S (2012) Ubiquitin-mediated regulation of endocytosis by proteins of the arrestin family. Biochem Res Int 2012: 242764.
34. Fukumoto H, Tomita T, Matsunaga H, Ishibashi Y, Saido TC, et al. (1999) Primary cultures of neuronal and non-neuronal rat brain cells secrete similar proportions of amyloid beta peptides ending at A beta40 and A beta42. Neuroreport 10: 2965–2969.
35. Suzuki K, Hayashi Y, Nakahara S, Kumazaki H, Prox J, et al. (2012) Activity-dependent proteolytic cleavage of neuroligin-1. Neuron 76: 410–422.
36. Karlstrom H, Bergman A, Lendahl U, Naslund J, Lundkvist J (2002) A sensitive and quantitative assay for measuring cleavage of presenilin substrates. The Journal of biological chemistry 277: 6763–6766.
37. Yamada K, Yabuki C, Seubert P, Schenk D, Hori Y, et al. (2009) Abeta immunotherapy: intracerebral sequestration of Abeta by an anti-Abeta monoclonal antibody 266 with high affinity to soluble Abeta. The Journal of neuroscience: the official journal of the Society for Neuroscience 29: 11393–11398.
38. Takabe K, Paugh SW, Milstien S, Spiegel S (2008) "Inside-out" signaling of sphingosine-1-phosphate: therapeutic targets. Pharmacol Rev 60: 181–195.
39. Lee MJ, Evans M, Hla T (1996) The inducible G protein-coupled receptor edg-1 signals via the G(i)/mitogen-activated protein kinase pathway. The Journal of biological chemistry 271: 11272–11279.
40. Mullershausen F, Craveiro LM, Shin Y, Cortes-Cros M, Bassilana F, et al. (2007) Phosphorylated FTY720 promotes astrocyte migration through sphingosine-1-phosphate receptors. Journal of neurochemistry 102: 1151–1161.
41. Wei SH, Rosen H, Matheu MP, Sanna MG, Wang SK, et al. (2005) Sphingosine 1-phosphate type 1 receptor agonism inhibits transendothelial migration of medullary T cells to lymphatic sinuses. Nature immunology 6: 1228–1235.
42. Miron VE, Jung CG, Kim HJ, Kennedy TE, Soliven B, et al. (2008) FTY720 modulates human oligodendrocyte progenitor process extension and survival. Ann Neurol 63: 61–71.
43. Ni Y, Zhao X, Bao G, Zou L, Teng L, et al. (2006) Activation of beta2-adrenergic receptor stimulates gamma-secretase activity and accelerates amyloid plaque formation. Nat Med 12: 1390–1396.
44. Tanaka S, Ishii K, Kasai K, Yoon SO, Saeki Y (2007) Neural expression of G protein-coupled receptors GPR3, GPR6, and GPR12 up-regulates cyclic AMP levels and promotes neurite outgrowth. J Biol Chem 282: 10506–10515.
45. Thathiah A, Spittaels K, Hoffmann M, Staes M, Cohen A, et al. (2009) The orphan G protein-coupled receptor 3 modulates amyloid-beta peptide generation in neurons. Science 323: 946–951.
46. Liu X, Zhao X, Zeng X, Bossers K, Swaab DF, et al. (2012) beta-Arrestin1 regulates gamma-secretase complex assembly and modulates amyloid-beta pathology. Cell Res.
47. Thathiah A, Horre K, Snellinx A, Vandewyer E, Huang Y, et al. (2012) beta-arrestin 2 regulates Abeta generation and gamma-secretase activity in Alzheimer's disease. Nat Med.
48. Lieven CJ, Ribich JD, Crowe ME, Levin LA (2012) Redox proteomic identification of visual arrestin dimerization in photoreceptor degeneration after photic injury. Invest Ophthalmol Vis Sci 53: 3990–3998.

49. Osawa S, Funamoto S, Nobuhara M, Wada-Kakuda S, Shimojo M, et al. (2008) Phosphoinositides suppress gamma-secretase in both the detergent-soluble and -insoluble states. J Biol Chem 283: 19283–19292.
50. Gomez-Raja J, Davis DA (2012) The beta-arrestin-like protein Rim8 is hyperphosphorylated and complexes with Rim21 and Rim101 to promote adaptation to neutral-alkaline pH. Eukaryot Cell 11: 683–693.
51. Shichita T, Sugiyama Y, Ooboshi H, Sugimori H, Nakagawa R, et al. (2009) Pivotal role of cerebral interleukin-17-producing gammadeltaT cells in the delayed phase of ischemic brain injury. Nature medicine 15: 946–950.
52. Kaneider NC, Lindner J, Feistritzer C, Sturn DH, Mosheimer BA, et al. (2004) The immune modulator FTY720 targets sphingosine-kinase-dependent migration of human monocytes in response to amyloid beta-protein and its precursor. FASEB J 18: 1309–1311.

Hoshi et al. BMC Biochemistry 2013, 14:16
http://www.biomedcentral.com/1471-2091/14/16

BMC Biochemistry

RESEARCH ARTICLE Open Access

Experimental detection of proteolytic activity in a signal peptide peptidase of *Arabidopsis thaliana*

Masako Hoshi[1], Yu Ohki[2], Keisuke Ito[3], Taisuke Tomita[2,4], Takeshi Iwatsubo[2,4,5], Yoshiro Ishimaru[1], Keiko Abe[1,6] and Tomiko Asakura[1*]

Abstract

Background: Signal peptide peptidase (SPP) is a multi-transmembrane aspartic protease involved in intramembrane-regulated proteolysis (RIP). RIP proteases mediate various key life events by releasing bioactive peptides from the plane of the membrane region. We have previously isolated *Arabidopsis* SPP (AtSPP) and found that this protein is expressed in the ER. An AtSPP-knockout plant was found to be lethal because of abnormal pollen formation; however, there is negligible information describing the physiological function of AtSPP. In this study, we have investigated the proteolytic activity of AtSPP to define the function of SPPs in plants.

Results: We found that an *n*-dodecyl-ß-maltoside (DDM)-solubilized membrane fraction from *Arabidopsis* cells digested the myc-Prolactin-PP-Flag peptide, a human SPP substrate, and this activity was inhibited by $(Z\text{-}LL)_2$-ketone, an SPP-specific inhibitor. The proteolytic activities from the membrane fractions solubilized by other detergents were not inhibited by $(Z\text{-}LL)_2$-ketone. To confirm the proteolytic activity of AtSPP, the protein was expressed as either a GFP fusion protein or solely AtSPP in yeast. SDS-PAGE analysis showed that migration of the fragments that were cleaved by AtSPP were identical in size to the fragments produced by human SPP using the same substrate. These membrane-expressed proteins digested the substrate in a manner similar to that in *Arabidopsis* cells.

Conclusions: The data from the *in vitro* cell-free assay indicated that the membrane fraction of both *Arabidopsis* cells and AtSPP recombinantly expressed in yeast actually possessed proteolytic activity for a human SPP substrate. We concluded that plant SPP possesses proteolytic activity and may be involved in RIP.

Keywords: Signal peptide peptidase (SPP), Endoplasmic reticulum (ER), Aspartic protease, Regulated intramembrane proteolysis (RIP), *Arabidopsis thaliana*

Background

Signal peptide peptidase (SPP) is a multi-transmembrane aspartic protease that contains two catalytic aspartates; the conserved YD and GXGD motifs in the sixth and seventh transmembrane domains, respectively [1]. SPP is located in the endoplasmic reticulum (ER) and the substrates of SPP are Type II membrane proteins, in which the locations of the N- and C-termini of these substrate proteins are in the cytosol and lumen, respectively. SPPs have been identified in human [1], mouse [2], zebrafish [3], fruit fly [4], *Caenorhabditis elegans* [5], *Arabidopsis thaliana* [6] and *Oryza sativa* [7]. Recessive lethal mutation studies of SPP in *Drosophila* indicated that SPP is necessary for development [4] and an SPP knockdown in zebrafish resulted in cell death in the central nervous system [3]. Moreover, a SPP knockdown in *C. elegans* led to embryonic death and an abnormal molting phenotype [5]. These data indicate that the SPP family is indispensable for survival. SPP appears to be involved in regulated intramembrane proteolysis through the cleavage of the substrate intramembrane region.

SPP promotes the intramembrane proteolysis of signal peptides following the cleavage of newly synthesized secretory or membrane proteins [8,9]. The resultant peptide fragments act as bioactive peptides that are liberated from the ER membrane. For example, the signal peptide fragments of human leukocyte antigens (HLA)-A liberated by

* Correspondence: asakura@mail.ecc.u-tokyo.ac.jp
[1]Department of Applied Biological Chemistry, Graduate School of Agricultural and Life Sciences, The University of Tokyo, 1-1-1 Yayoi, Bunkyo-ku, Tokyo 113-8657, Japan
Full list of author information is available at the end of the article

SPP bind to HLA-E molecules and are subsequently presented to NK-cells for immune surveillance [10,11].

The secretory protein hormone preprolactin is also processed by SPP and the resulting N-terminal fragments are released into the cytosol [8]. Thereafter, the fragments bind to calmodulin and enter into the cellular signal transduction pathway [12]. In addition, SPP participates in the maturation of the core protein of the hepatitis C virus (HCV) [13]. SPP also possesses non-enzymatic functions, including molecular chaperone activity. SPP interacts with the human cytomegalovirus glycoprotein US2 and induces the dislocation of MHC class I heavy chains to the proteasome system [14]. Moreover, based on the observation that SPP interacts with newly synthesized membrane proteins *in vitro*, human SPP (HsSPP) interacts with signal peptides and misfolded membrane proteins that are removed during ER quality control. However, SPP does not interact with all types of membrane proteins [15]. Thus, the function of mammalian SPP has been examined, yet there are only a few studies that have examined plant SPPs. We have previously isolated AtSPP (At2g03120) in *Arabidopsis thaliana*, and have shown that AtSPP is strongly expressed in the shoot meristem of germination seeds and in the inflorescence meristem during the reproductive stage [6]. We have investigated a GFP-fused AtSPP protein in cultured "Deep" cells and found that this protein is localized in the ER. Moreover, subcellular localization studies of endogenous AtSPP in "Deep" cells by equilibrium sucrose density gradient centrifugation also indicated that AtSPP is localized in the ER [6]. The shoot meristem contains undifferentiated cells that have the potential to differentiate into all aerial parts of the plant [6]. Based on these results, it is conceivable that AtSPP is involved in regulating growth and differentiation in *Arabidopsis*. This notion is supported by a knockout of the AtSPP gene giving rise to a lethal phenotype [16]. However, the target molecule of SPP in plants remains unresolved. Recently, it was reported that nodule-specific cysteine rich polypeptides (NCR) mediate consecutive differentiation events with symbiosomes in *Medicago truncatula* [17]. NCR propeptides are likely to be processed by the signal peptidase complex (SPC) and converted to the active form. The highly correlated expression of SPC with SPP suggests that NCR signal peptides can be processed by SPP [18,19]. To reveal the function of plant SPPs, it is important to examine the proteolytic activity of SPPs.

Herein, we present evidence that the SPP of *Arabidopsis* actually possesses proteolytic activity, suggesting that the plant SPP cleaves the target proteins in the membrane and releases bioactive peptides that function in signal transduction pathways, similar to the phenomena observed for other species.

Results

Preparation of the membrane fraction of "deep" cell extracts and the proteolytic activity of this fraction

For the purposes of studying the proteolytic activity of AtSPP, we have isolated the membrane fraction of *Arabidopsis* root derived cultured "Deep" cells. The AtSPP protein was detected by SDS-PAGE as a single band in the membrane fraction of "Deep" cells (Figure 1A). The deduced size of the protein estimated from the primary sequence was 38 kDa. The band representing AtSPP migrated further on the SDS-PAGE than the estimated molecular weight. Nonetheless, such anomalous electrophoretic migration has been shown previously for ER fractions isolated from "Deep" cells [6].

Several detergents were tested for their suitability to solubilize active AtSPP from the membranes. Digitonin, CHAPS-, CHAPSO- and NP-40-solubilized membrane

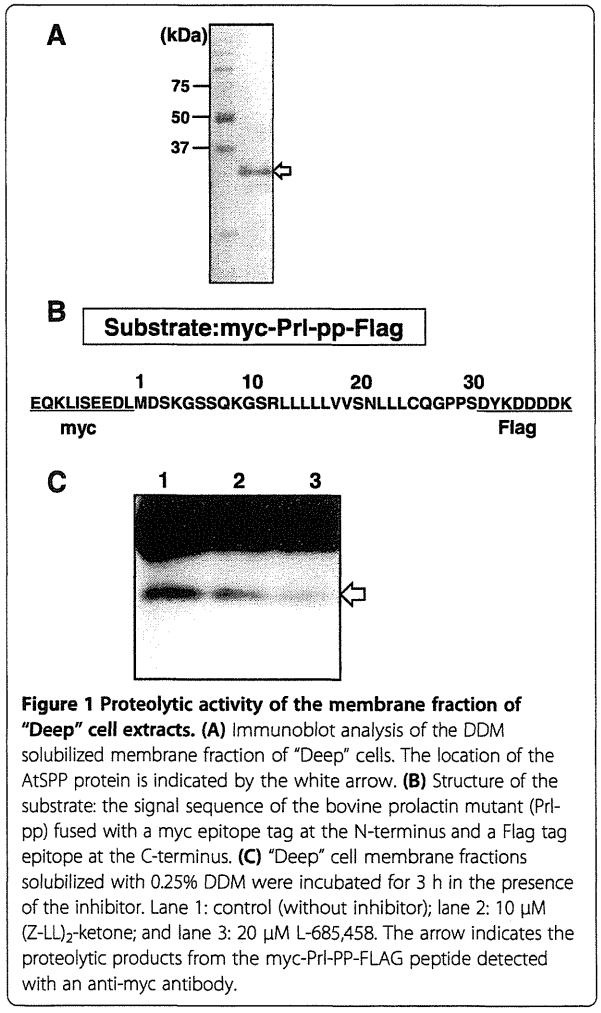

Figure 1 Proteolytic activity of the membrane fraction of "Deep" cell extracts. (A) Immunoblot analysis of the DDM solubilized membrane fraction of "Deep" cells. The location of the AtSPP protein is indicated by the white arrow. **(B)** Structure of the substrate: the signal sequence of the bovine prolactin mutant (Prl-pp) fused with a myc epitope tag at the N-terminus and a Flag tag epitope at the C-terminus. **(C)** "Deep" cell membrane fractions solubilized with 0.25% DDM were incubated for 3 h in the presence of the inhibitor. Lane 1: control (without inhibitor); lane 2: 10 μM $(Z\text{-}LL)_2$-ketone; and lane 3: 20 μM L-685,458. The arrow indicates the proteolytic products from the myc-Prl-PP-FLAG peptide detected with an anti-myc antibody.

fractions were examined for their activity to digest the synthetic peptide myc-Prl-PP-Flag [20] (Figure 1B). Although all of these membrane fractions showed proteolytic activities, none were inhibited by the SPP-specific inhibitor $(Z\text{-}LL)_2$-ketone (data not shown). This indicates that the proteolytic activity of the membrane fraction was induced by proteases other than SPP. We then tested whether an *n*-dodecyl-ß-maltoside (DDM)-solubilized membrane fraction showed proteolytic activity, because human SPP has been shown to exhibit proteolytic activity using this preparation [20]. As shown in Figure 1C, this fraction (0.079 μg of protein) actively cleaved the myc-Prl-PP-Flag peptide and was inhibited by $(Z\text{-}LL)_2$-ketone, as well as L-685,458, an aspartic protease inhibitor that targets SPP or presenilin [21]. Based on these results, we concluded that the DDM-solubilized membrane fraction possesses SPP-like proteolytic activity, and likely has activity from other proteases.

AtSPP-GFP fusion protein expression in *Saccharomyces cerevisiae*

To determine whether the proteolytic activity of the DDM-solubilized "Deep" cell membrane fraction was

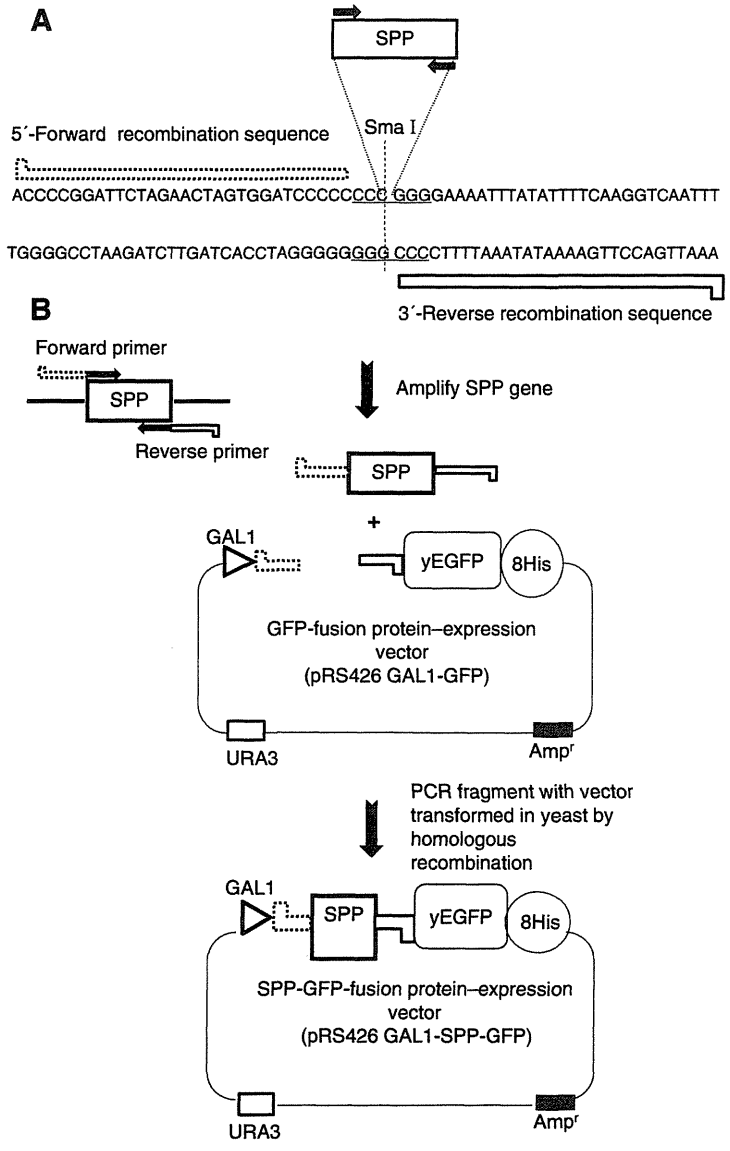

Figure 2 Construction of GFP-fusion protein expression plasmid. (A) Cloning site of pRS426 GAL1-GFP and overlapping recombination sequence of the primer. **(B)** SPP genes were amplified with primers described in the Materials and Methods. The *Sma*I digested vector and PCR products were transformed into *Saccharomyces cerevisiae* by homologous recombination. yEGFP stands for enhanced green fluorescent protein.

indeed caused by AtSPP, we expressed an AtSPP GFP-fusion protein (AtSPP-GFP) in yeast cells, as described previously [22]. As shown in Figure 2, the linearized vector (pRS426- GAL1-GFP) and amplified PCR products were transformed into *S. cerevisiae* BY2777. Figure 3 shows the confocal microscopy image of HsSPP-GFP and AtSPP-GFP localization. Yeast cells transformed with the vector alone did not exhibit any GFP fluorescence; however, fluorescence was detected in the HsSPP-GFP- and AtSPP-GFP-transformed cells. These results indicate that the AtSPP-GFP fusion protein was successfully expressed. We next confirmed the expression of the fusion proteins by in-gel fluorescence. Yeast cells were separated into soluble and membrane-bound fractions after mechanical disruption. Fluorescent bands of GFP-fusion proteins are shown in Figure 4A. No band was detected in the soluble fraction. The 2% DDM-solubilized membrane fraction band is indicated by the white arrowheads. Moreover, the intensity of the AtSPP-GFP band increased in a dose-dependent manner (Figure 4A). These data suggest that AtSPP-GFP and HsSPP-GFP are localized in the yeast membrane fraction. Based on their primary sequences, the sizes of AtSPP-GFP and HsSPP-GFP are estimated to be 65 and 72 kDa, respectively. AtSPP-GFP migrated at a size smaller than 65 kDa, whereas HsSPP-GFP migrated at a size more than 72 kDa. While the reasons underlying this anomalous migration remain to be elucidated, previous Blue Native Polyacrylamide Gel Electrophoresis (BN-PAGE) studies have shown that HsSPP forms a high molecular mass complex under DDM-solubilized conditions [23]. HsSPP and AtSPP may assemble into complexes of different molecular masses.

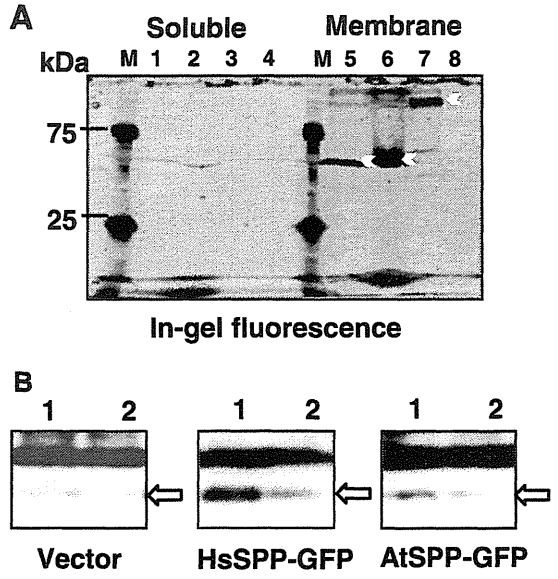

Figure 4 Expression of the SPP-GFP fusion protein in yeast. **(A)** Soluble and membrane fractions were analyzed by 12% SDS-PAGE using in-gel fluorescence. The protein concentrations loaded were as follows: Soluble fractions in the left panel; lane 1, AtSPP-GFP, 117 μg; lane 2, AtSPP-GFP, 340 μg; lane 3, HsSPP-GFP, 56 μg; and lane 4, vector, 56 μg. Membrane fractions in the right panel: lane 5, AtSPP-GFP, 306 μg; lane 6, AtSPP-GFP, 1120 μg; lane 7, HsSPP-GFP, 158 μg; and lane 8, vector, 161 μg. Detection of GFP fluorescence in the gel was carried out by exposure to blue light (EPI) at 460 nm with a cut-off filter. The arrows indicate the location of the GFP fusion proteins. **(B)** Proteolytic activity of the membrane fraction of GFP-fusion protein. Solubilized membrane fractions of yeast cells overexpressing the vector control (183.1 μg) HsSPP-GFP (197.5 μg) and AtSPP-GFP (55 μg) proteins were incubated for 15 h in the presence or absence of the inhibitor. Lane 1: control (without inhibitor); and lane 2: 50 μM $(Z\text{-}LL)_2$-ketone. Arrows indicate the proteolytic products from myc-Prl-PP-FLAG detected with the anti-myc antibody.

In vitro cell-free assay using AtSPP overexpressed in yeast

Next, the membrane fractions containing GFP-fusion proteins were examined for proteolytic activity using an *in vitro* assay system. Both HsSPP-GFP and AtSPP-GFP exhibited proteolytic activity in the *in vitro* assay. Faint bands were detected in the lanes of the vector control. However, this band was not inhibited by the $(Z\text{-}LL)_2$-ketone. This cleavage was due to an intrinsic proteinase present in yeast. Though the rate of proteolytic activity of AtSPP-GFP was weak, the activity was inhibited by the $(Z\text{-}LL)_2$-ketone, an SPP-specific inhibitor (Figure 4B). Our results suggest that the AtSPP-GFP fusion protein possesses proteolytic activity.

To confirm the proteolytic activity of AtSPP, we expressed AtSPP without the GFP protein, thereby creating a protein construct that is closer to the native form. DDM-solubilized yeast membrane fractions were extracted and AtSPP was detected by immunoblotting using an anti-AtSPP antibody (Figure 5A). The arrowheads indicate the bands which specifically cross-reacted with the anti-AtSPP antibody. The overexpressed AtSPP

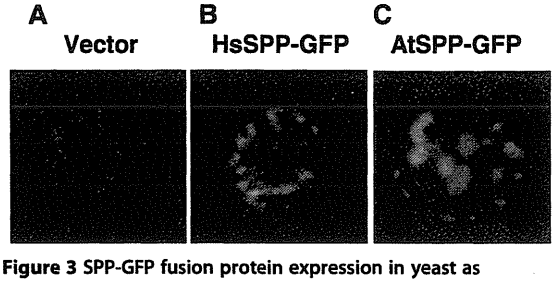

Figure 3 SPP-GFP fusion protein expression in yeast as visualized by confocal microscopy. An aliquot of the yeast culture cell suspension overexpressing the fusion protein was placed onto a microscope slide to observe GFP fluorescence by microscopy. **(A)** Fluorescence from the control cells harboring only the vector. GFP fluorescence was not detected. **(B)** Transformation with HsSPP-GFP. **(C)** Transformation with AtSPP-GFP.

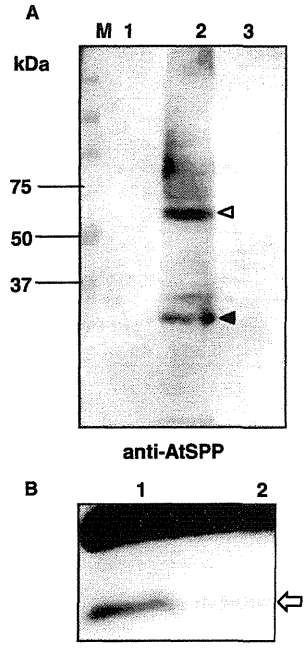

Figure 5 Identification of the proteolytic activity by overexpressing AtSPP in yeast. (A) Immunoblot analysis of DDM-solubilized membrane fraction overexpressing AtSPP in yeast by using anti-AtSPP. Lane 1, vector control; lane 2, overexpression of AtSPP in yeast; and lane 3, overexpression of HsSPP-GFP in yeast. The filled-arrowhead indicates the monomer and the open-arrowhead indicates the dimer. **(B)** Evaluation of the proteolytic activity of AtSPP overexpressed in yeast. Proteolytic activity of the membrane fraction of yeast cells overexpressing AtSPP with inhibitor. Lane 1: control (without inhibitor); lane 2: 1 μM$(Z\text{-}LL)_2$ small capitor-ketone. The arrow indicates the proteolytic products from myc small capitor-Prl-PP-FLAG peptide detected with the anti-myc antibody.

detected in yeast was identified in the gel analysis by two bands. Electrophoretic migration of AtSPP in "Deep" cells (Figure 1A) matched the lower band detected in the yeast sample. Therefore, the lower molecular weight band may be a monomeric species and the higher molecular weight band may represent a dimer that is not affected by SDS treatment.

No bands were detected in the control vector (Figure 5A, lane 1) and the HsSPP-GFP-transformed cell samples (Figure 5A, lane 3). The proteolytic activity of AtSPP in the presence of the $(Z\text{-}LL)_2$-ketone is shown in Figure 5B. The proteolytic activity toward myc-Prl-PP-FLAG is almost completely inhibited by 1 μM $(Z\text{-}LL)_2$-ketone. In summary, our results confirm that AtSPP proteolytically cleaves the myc-Prl-PP-FLAG substrate *in vitro*.

Comparison of the cleavage site of myc-Prl-PP-FLAG using electrophoresis

Electrophoresis of the fragments from myc-Prl-PP-FLAG was carried out and detected by an anti-myc antibody. A MALDI-TOF mass spectrometry study showed that human SPP cleaved primarily at a single site between Leu-23 and Leu-24 [17]. To compare the main cleavage sites, fragments from myc-Prl-PP-FLAG cleaved by various SPPs were co-electrophoresed with a synthesized marker fragment of Prl-23 (Figure 6A) on a Tris/Tricine urea gel. Figure 6 shows that HEK293T cells expressing native human SPP cleaved myc-Prl-PP-FLAG at the C-terminal of Leu-23 and the SPP was inhibited by the $(Z\text{-}LL)_2$-ketone. The fragment arising from the digestion of the synthetic Prl-23 by the overexpressed HsSPP-GFP fusion protein, membrane fraction of "Deep" cells and recombinant AtSPP migrated to the same location (Figure 6B). This result indicates that AtSPP cleaved mainly myc-Prl-PP-FLAG at the same sequence as the human SPP did.

Discussion

We have detected the AtSPP protein in a membrane fraction of "Deep" cells (Figure 1A). The proteolytic activity of the DDM-solubilized "Deep" cell membrane fraction was blocked by the $(Z\text{-}LL)_2$-ketone and L-685,458 inhibitors (Figure 1C). These results confirm that SPP exists in the membrane fraction of "Deep" cells; however, the result also indicates that an aspartic protease other than SPP exists in this fraction. Proteolytic activity of SPP was detected in the DDM-solubilized membrane fraction, but not in the other detergent-solubilized membrane fractions prepared. Previous studies have shown

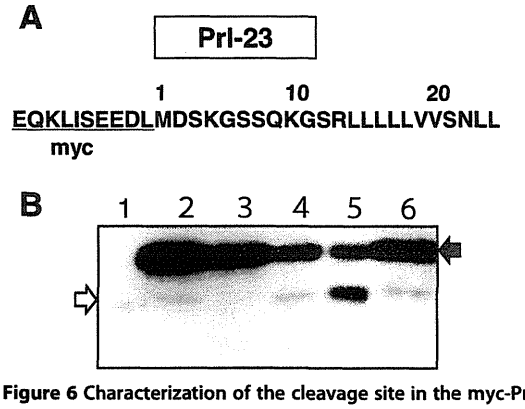

Figure 6 Characterization of the cleavage site in the myc-Prl-PP-FLAG peptide. Products of the myc-Prl-PP-FLAG peptide proteolysis by various SPP proteins and standard peptides Prl-23 were separated by a Tris/Tricine urea gel and detected with an anti-myc antibody. **(A)** Structure of the substrate Prl-23: Prl-23 is a N-terminal fragment of myc-Prl-PP-FLAG peptide composed of 23 amino acid residues. **(B)** Lane 1, synthesized marker fragment of Prl-23; lane 2, the membrane fraction of HEK293T cells; lane 3, HEK293T cells with 10 μM $(Z\text{-}LL)_2$-ketone inhibitor; lane 4, membrane fraction of yeast cells overexpressing HsSPP-GFP; lane 5, membrane fraction of "Deep" cell extracts; lane 6, the membrane fraction of yeast cells overexpressing AtSPP. The black arrow indicates myc-Prl-PP-FLAG as the original peptide and the white arrow indicates the position of the proteolytic fragment.

that the γ-secretase complex dissociates in DDM [24] and thus, γ-secretase should not be active in the DDM solubilized membrane fraction. Therefore, the difference in the extent of inhibition brought about by $(Z\text{-}LL)_2$-ketone and L-685,458 may be due to the presence of an aspartic protease other than γ-secretase. AtSPP and AtSPP-GFP fusion proteins were successfully sorted toward the membrane fraction and were expressed in *S. cerevisiae*. Moreover, expressed AtSPP was observed to cleave the substrate myc-Prl-PP-Flag.

We have observed proteolytic activity of endogenous SPP in human HEK293T cells (Figure 6B). Similarly, the proteolytic activity of the HsSPP-GFP fusion protein overexpressed in yeast was found to efficiently process preprolactin, because the preprolactin sequence is derived from mammals. The signal sequences have some common features, although there are no apparent common sequences [25]. The signal sequence consists of a tripartite structure: a central hydrophobic h-region, a positively charged hydrophilic n-region and a C-terminal flanking polar region. The h-region often contains helix-breaking amino acids, such as glycine, proline, tyrosine and serine. The central hydrophobic h-region of the preprolactin signal sequence also has helix-destabilizing serine and asparagine residues. Although the preprolactin sequence is not a native substrate of the plant SPP, we have identified that AtSPP can cleave at the typical position after the helix-breaking amino acids in the central hydrophobic h-region, in a similar manner to that in which human SPP cleaves preprolactin.

Immunoblot analysis of the DDM-solubilized membrane fraction from the AtSPP-overexpressing yeast cells using an anti-AtSPP antibody detected two bands (Figure 5A). In contrast, the DDM-solubilized "Deep" cell membrane fraction extracted by the same method detected only one band (Figure 1A). Recently, Miyashita et al. [23] suggested that the proteolytic activity of *Drosophila* SPP requires its assembly into high molecular weight complexes. HsSPP was also reported to assemble into oligomeric complexes [26]. HsSPP can be isolated both as a monomer and as an SDS-stable dimer. Under denaturing conditions, AtSPP was isolated as a monomer in the "Deep" cell sample and as a SDS-resistant dimer when overexpressed in yeast. Thus, it is possible that AtSPP may assemble into both oligomeric complexes and monomer under native conditions.

A previous paper showed that the sequence homology around the active site motifs YD, GLGD and PAL is highly conserved [1]. In contrast, the sequence of the N-terminus of AtSPP and the transmembrane region 1 (TM1) differs noticeably when compared with the sequences from other species. Although the topological conformation to face the membrane is reversed, the active site and PAL motif of human SPP and presenilin are identical, suggesting a common catalytic mechanism. The structural analysis of the initial substrate binding site by γ-secretase modulators (GSMs) showed GSMs bind directly to the TM1 of PS and affect the structure of the catalytic site [27]. Human SPP was also affected by non-steroidal anti-inflammatory drugs (NSAIDs) that function as GSMs [20]. These data suggest a crucial role of the TM1 in the intramembrane cleaving mechanism. It is very interesting that AtSPP possessing a different TM1 cleaved the same substrates as human SPP. Hereafter, unraveling how the digestion occurs by modification experiments in the TM1 region of AtSPP is required.

Currently, the native substrates targeted by SPP in plants have not been identified. Further investigation of these substrates is needed for understanding the function of SPPs in plants. Research detailing the native substrates and the role of SPPs in the plant life cycle is in progress.

Conclusion

"Deep" cells possess a signal peptide peptidase with proteolytic activity.

AtSPP and AtSPP-GFP were expressed in the membrane fraction of *S. cerevisiae* and shown to digest the HsSPP substrate. The activities of AtSPP and AtSPP-GFP were inhibited in the presence of an SPP-specific inhibitor. The main cleavage site of AtSPP was identified as identical to the site in human SPP. We conclude that plant SPPs possess proteolytic activity, and that this activity is likely to be involved in RIP.

Methods

Materials and cell culture

Myc-Prl-PP-Flag [28] was synthesized by BEX Co., LTD. (Tokyo, Japan) with the sequence illustrated in Figure 1B. Prl-23 was also synthesized by BEX Co., LTD. (Tokyo, Japan) with the sequence illustrated in Figure 6A. [(2*R*,4*R*,5*S*)-2-Benzyl-5-(*t*-butyloxycarbonylamino)-4-hydroxy-6-phenylhexanoyl]-L-leucyl-L-phenylalanine amide (L-685,458) [29] and 1,3-di-(*N*-carboxybenzoyl-L-leucyl-L-leucyl) amino acetone ($(Z\text{-}LL)_2$-ketone) [30] were purchased from Calbiochem (San Diego, CA. USA) and PEPTIDE INSTITUTE INC. (Osaka, Japan), respectively.

Arabidopsis root cells ("Deep" cells) were cultured at 22°C in Murashige and Skoog medium under dark conditions. The rabbit polyclonal anti-AtSPP C terminus antibody was obtained as described previously [6]. The rabbit anti-c-myc polyclonal antibody was purchased from Sigma-Aldrich (St. Louis, MO, USA).

Extraction of membrane fractions and immunoblotting

The extraction of membrane fractions was carried out as described previously [20]. Briefly, a "Deep" cell suspension culture (100 ml) was centrifuged and the pellet was collected. The cells were homogenized in (H) buffer (50 mM HEPES, pH 7.0, 250 mM sucrose, 5 mM EDTA) containing a complete protease inhibitor cocktail (Roche,

Basel, Switzerland). The cells were disrupted using a French press at 1,000 psi and centrifuged at 3,000 × *g* for 10 min to remove cell debris and nuclei. The supernatant was centrifuged again at 100,000 × *g* for 60 min to isolate the microsomal fraction. Microsome pellets were resuspended in 2% DDM-containing (H) buffer for 90 min on ice, and then centrifuged at 25,000 × *g* for 15 min. The solubilized membrane fraction was passed through an Amicon Ultra-0.5 centrifugal filter device-10 K (Millipore, Tokyo, Japan) and then diluted for the assay. Yeasts were cultured at 30°C for 22 h after induction by galactose. The cells were collected and harvested using a Multi-beads shocker (Yasui Kikai, Osaka, Japan). Human embryonic kidney (HEK) 293 T cells were incubated in Dulbecco's modified Eagle's medium (DMEM, Sigma Aldrich, St. Louis, MO, USA) supplemented with 10% fetal bovine serum (Invitrogen, Carlsbad, CA, USA) at 37°C under 5% CO_2 and were collected and harvested using a French press at 1,000 psi. The membrane fractions of yeasts and HEK 293 T cells were obtained in a similar manner to the process used for *Arabidopsis* cells after harvesting. SDS-PAGE and immunoblotting were performed as described previously [6].

Expression of GFP-fusion SPP in *Saccharomyces cerevisiae*

The GFP-fused protein-expression vector (pRS426 GAL1-GFP) [22] was kindly provided by Dr. Iwata (Imperial College, London). The *S. cerevisiae* BY2777 (MATa prb1-1122 prc1-407 pep4-3 ura3-52 leu2 trp1) strain was provided by the National Bio-Resource Project (NBRP), MEXT, Japan. This plasmid was composed of a C-terminal yeast-enhanced green fluorescent protein (yEGFP), which is lacking the N-terminal methionine, fused with an octa-His tag, and harbors a GAL1 promoter and URA selection marker (Figure 2). The SPP protein sequence, lacking a stop codon, was inserted into the reverse primer for GFP expression. DNA was amplified with the following primer pair: HsSPP forward primer (5′-accccggattctagaactagtggatcccccatggactcggcc ctcagcgatc-3′) and reverse primer (5′-aaattgaccttgaaaata taaattttcccctttctctttcttctccagccccttc-3′). AtSPP-GFP forward primer (5′-accccggattctagaactagtggatcccccatgaag aattgtgagagatttgc-3′) and reverse primer (5′-aaatt gaccttgaaaatataaattttcccctttcatcatgagctttattaacctc-3′). For studying the expression of the protein without GFP, another reverse primer was prepared, the AtSPP reverse primer, (5′-aaattgaccttgaaaatataaattttcccctcattcatcatgagc tttattaacc-3′) (Figure 2).

The expression plasmids were constructed as follows: the expression vector (pRS426 GAL1-GFP) was linearized with *Sma*I and the amplified fragment was inserted by homologous recombination using Frozen-EZ Yeast Transformation II (Zymo Research, Irvine, CA, USA). The transformants were selected by growing in the absence of the uracil medium, as described previously [22]. The expression of SPP-GFP was confirmed by confocal microscopy (FV10i-LIV, Olympus Tokyo Japan). In-gel fluorescence was performed using an Image Quant LAS-4000mini (GE Healthcare, Amersham, Uppsala, Sweden).

In vitro cell-free assay

Membrane fractions solubilized by 0.25% DDM were incubated at 37°C with 1 μM of the myc-Prl-PP-FLAG peptide (BEX Co., Ltd., Tokyo, Japan) containing a protease inhibitor cocktail (Roche, Basel, Switzerland) for the appropriate times. For the inhibitor assay, the reaction mixtures were incubated in the presence or absence of the $(Z\text{-}LL)_2$-ketone), a SPP inhibitor, and L-685,458, an aspartic protease inhibitor. Dimethyl sulfoxide was used as a vehicle control. Products were separated on a 15% Tris/Tricine SDS gel containing 8 M urea, then transferred to a 0.2-μm polyvinylidene difluoride membrane (Whatman, Maidstone, UK), and detected with an anti-c-myc antibody. Signal detection was performed with the Image Quant LAS-4000mini (GE Healthcare) using the ECL system (GE Healthcare).

Abbreviations

SPP: Signal peptide peptidase; ER: Endoplasmic reticulum; RIP: Regulated intramembrane proteolysis; HEK: Human embryonic kidney; CBB: Coomassie brilliant blue; DDM: *n*-dodecyl-ß-maltoside; NK-cell: Natural killer cells; MHC: Major histocompatibility complex; HLA: Human leukocyte antigens; NCR: Nodule-specific cysteine rich; SPC: Signal peptidase complex; GFP: Green fluorescent protein; GSMs: γ-secretase modulators; NSAIDs: Non-steroidal anti-inflammatory drugs; PS: Presenilin.

Competing interests

The authors declare that they have no competing interests.

Authors' contributions

MH, KA and TA designed the research. MH performed all the research. YO and KI constructed the enzyme assay and yeast expression system, respectively. TT analyzed the data. MH, YO, KI, TT, TI, YI, KA and TA wrote the paper. All authors read and approved the final manuscript.

Acknowledgements

We thank Dr. Sato (Eisai Ltd.) for helpful discussions and technical assistance. We also thank Dr. Maeda (The University of Tokyo) for the help in yeast handling. We are grateful to Dr. Iwata (Imperial College, London) for providing us with the pRS426-GAL1-GFP vector. This work was supported by Nissin Food Products Co. and the Salt Science Research Foundation (Grant 11D1).

Author details

[1]Department of Applied Biological Chemistry, Graduate School of Agricultural and Life Sciences, The University of Tokyo, 1-1-1 Yayoi, Bunkyo-ku, Tokyo 113-8657, Japan. [2]Department of Neuropathology and Neuroscience, Graduate School of Pharmaceutical Sciences, The University of Tokyo, 7-3-1 Hongo, Bunkyo-ku, Tokyo 113-0033, Japan. [3]Department of Food and Nutritional Sciences, Graduate School of Nutritional and Environmental Sciences, University of Shizuoka, 52-1 Yada, Suruga-ku, Shizuoka 442-8802, Japan. [4]Core Research for Evolutional Science and Technology, Japan Science and Technology Agency, 7-3-1 Hongo, Bunkyo-ku, Tokyo 113-0033, Japan. [5]Department of Neuropathology, Graduate School of Medicine, The University of Tokyo, 7-3-1 Hongo, Bunkyo-ku, Tokyo 113-0033, Japan. [6]Food Safety and Reliability Project, Kanagawa Academy of Science and Technology, 3-2-1 Sakado, Takatsu-ku, Kawasaki 213-0012, Japan.

Received: 5 December 2012 Accepted: 2 July 2013
Published: 6 July 2013

References

1. Weihofen A, Binns K, Lemberg MK, Ashman K, Martoglio B: **Identification of signal peptide peptidase, a presenilin-type aspartic protease.** *Science* 2002, **296**(5576):2215–2218.
2. Urny J, Hermans-Borgmeyer I, Gercken G, Schaller HC: **Expression of the presenilin-like signal peptide peptidase (SPP) in mouse adult brain and during development.** *Gene Expr Patterns* 2003, **3**(5):685–691.
3. Krawitz P, Haffner C, Fluhrer R, Steiner H, Schmid B, Haass C: **Differential localization and identification of a critical aspartate suggest non-redundant proteolytic functions of the presenilin homologues SPPL2b and SPPL3.** *J Biol Chem* 2005, **280**(47):39515–39523.
4. Casso DJ, Tanda S, Biehs B, Martoglio B, Kornberg TB: **Drosophila signal peptide peptidase is an essential protease for larval development.** *Genetics* 2005, **170**(1):139–148.
5. Grigorenko AP, Moliaka YK, Soto MC, Mello CC, Rogaev EI: **The Caenorhabditis elegans IMPAS gene, imp-2, is essential for development and is functionally distinct from related presenilins.** *Proc Natl Acad Sci USA* 2004, **101**(41):14955–14960.
6. Tamura T, Asakura T, Uemura T, Ueda T, Terauchi K, Misaka T, Abe K: **Signal peptide peptidase and its homologs in Arabidopsis thaliana–plant tissue-specific expression and distinct subcellular localization.** *FEBS J* 2008, **275**(1):34–43.
7. Tamura T, Kuroda M, Oikawa T, Kyozuka J, Terauchi K, Ishimaru Y, Abe K, Asakura T: **Signal peptide peptidases are expressed in the shoot apex of rice, localized to the endoplasmic reticulum.** *Plant Cell Rep* 2009, **28**(11):1615–1621.
8. Lyko F, Martoglio B, Jungnickel B, Rapoport TA, Dobberstein B: **Signal sequence processing in rough microsomes.** *J Biol Chem* 1995, **270**(34):19873–19878.
9. Klappa P, Dierks T, Zimmermann R: **Cyclosporin A inhibits the degradation of signal sequences after processing of presecretory proteins by signal peptidase.** *Eur J Biochem* 1996, **239**(2):509–518.
10. Braud VM, Allan DS, O'Callaghan CA, Söderström K, D'Andrea A, Ogg GS, Lazetic S, Young NT, Bell JI, Phillips JH, *et al*: **HLA-E binds to natural killer cell receptors CD94/NKG2A, B and C.** *Nature* 1998, **391**(6669):795–799.
11. Lemberg MK, Bland FA, Weihofen A, Braud VM, Martoglio B: **Intramembrane proteolysis of signal peptides: an essential step in the generation of HLA-E epitopes.** *J Immunol* 2001, **167**(11):6441–6446.
12. Martoglio B, Graf R, Dobberstein B: **Signal peptide fragments of preprolactin and HIV-1 p-gp160 interact with calmodulin.** *EMBO J* 1997, **16**(22):6636–6645.
13. McLauchlan J, Lemberg MK, Hope G, Martoglio B: **Intramembrane proteolysis promotes trafficking of hepatitis C virus core protein to lipid droplets.** *EMBO J* 2002, **21**(15):3980–3988.
14. Loureiro J, Lilley BN, Spooner E, Noriega V, Tortorella D, Ploegh HL: **Signal peptide peptidase is required for dislocation from the endoplasmic reticulum.** *Nature* 2006, **441**(7095):894–897.
15. Schrul B, Kapp K, Sinning I, Dobberstein B: **Signal peptide peptidase (SPP) assembles with substrates and misfolded membrane proteins into distinct oligomeric complexes.** *Biochem J* 2010, **427**(3):523–534.
16. Han S, Green L, Schnell DJ: **The signal peptide peptidase is required for pollen function in Arabidopsis.** *Plant Physiol* 2009, **149**(3):1289–1301.
17. Mergaert P, Nikovics K, Kelemen Z, Maunoury N, Vaubert D, Kondorosi A, Kondorosi E: **A novel family in Medicago truncatula consisting of more than 300 nodule-specific genes coding for small, secreted polypeptides with conserved cysteine motifs.** *Plant Physiol* 2003, **132**(1):161–173.
18. Van de Velde W, Zehirov G, Szatmari A, Debreczeny M, Ishihara H, Kevei Z, Farkas A, Mikulass K, Nagy A, Tiricz H, *et al*: **Plant peptides govern terminal differentiation of bacteria in symbiosis.** *Science* 2010, **327**(5969):1122–1126.
19. Wang D, Griffitts J, Starker C, Fedorova E, Limpens E, Ivanov S, Bisseling T, Long S: **A nodule-specific protein secretory pathway required for nitrogen-fixing symbiosis.** *Science* 2010, **327**(5969):1126–1129.
20. Sato T, Nyborg AC, Iwata N, Diehl TS, Saido TC, Golde TE, Wolfe MS: **Signal peptide peptidase: biochemical properties and modulation by nonsteroidal antiinflammatory drugs.** *Biochemistry* 2006, **45**(28):8649–8656.
21. Friedmann E, Lemberg MK, Weihofen A, Dev KK, Dengler U, Rovelli G, Martoglio B: **Consensus analysis of signal peptide peptidase and homologous human aspartic proteases reveals opposite topology of catalytic domains compared with presenilins.** *J Biol Chem* 2004, **279**(49):50790–50798.
22. Drew D, Newstead S, Sonoda Y, Kim H, von Heijne G, Iwata S: **GFP-based optimization scheme for the overexpression and purification of eukaryotic membrane proteins in Saccharomyces cerevisiae.** *Nat Protoc* 2008, **3**(5):784–798.
23. Miyashita H, Maruyama Y, Isshiki H, Osawa S, Ogura T, Mio K, Sato C, Tomita T, Iwatsubo T: **Three-dimensional structure of the signal peptide peptidase.** *J Biol Chem* 2011, **286**(29):26188–26197.
24. Fraering PC, LaVoie MJ, Ye W, Ostaszewski BL, Kimberly WT, Selkoe DJ, Wolfe MS: **Detergent-dependent dissociation of active gamma-secretase reveals an interaction between Pen-2 and PS1-NTF and offers a model for subunit organization within the complex.** *Biochemistry* 2004, **43**(2):323–333.
25. von Heijne G: **Signal sequences. The limits of variation.** *J Mol Biol* 1985, **184**(1):99–105.
26. Schröder B, Saftig P: **Molecular insights into mechanisms of intramembrane proteolysis through signal peptide peptidase (SPP).** *Biochem J* 2010, **427**(3):e1–e3.
27. Ohki Y, Higo T, Uemura K, Shimada N, Osawa S, Berezovska O, Yokoshima S, Fukuyama T, Tomita T, Iwatsubo T: **Phenylpiperidine-type γ-secretase modulators target the transmembrane domain 1 of presenilin 1.** *EMBO J* 2011, **30**(23):4815–4824.
28. Lemberg MK, Martoglio B: **Requirements for signal peptide peptidase-catalyzed intramembrane proteolysis.** *Mol Cell* 2002, **10**(4):735–744.
29. Shearman MS, Beher D, Clarke EE, Lewis HD, Harrison T, Hunt P, Nadin A, Smith AL, Stevenson G, Castro JL: **L-685,458, an aspartyl protease transition state mimic, is a potent inhibitor of amyloid beta-protein precursor gamma-secretase activity.** *Biochemistry* 2000, **39**(30):8698–8704.
30. Weihofen A, Lemberg MK, Ploegh HL, Bogyo M, Martoglio B: **Release of signal peptide fragments into the cytosol requires cleavage in the transmembrane region by a protease activity that is specifically blocked by a novel cysteine protease inhibitor.** *J Biol Chem* 2000, **275**(40):30951–30956.

doi:10.1186/1471-2091-14-16
Cite this article as: Hoshi *et al.*: Experimental detection of proteolytic activity in a signal peptide peptidase of *Arabidopsis thaliana*. *BMC Biochemistry* 2013 **14**:16.

Ohki et al. Molecular Neurodegeneration 2014, 9:7
http://www.molecularneurodegeneration.com/content/9/1/7

MOLECULAR NEURODEGENERATION

RESEARCH ARTICLE Open Access

Binding of longer Aβ to transmembrane domain 1 of presenilin 1 impacts on Aβ42 generation

Yu Ohki[1], Naoaki Shimada[2], Aya Tominaga[1], Satoko Osawa[1], Takuya Higo[2], Satoshi Yokoshima[2,3], Tohru Fukuyama[2,3], Taisuke Tomita[1,4*] and Takeshi Iwatsubo[1,4,5]

Abstract

Background: Amyloid-β peptide ending at 42nd residue (Aβ42) is believed as a pathogenic peptide for Alzheimer disease. Although γ-secretase is a responsible protease to generate Aβ through a processive cleavage, the proteolytic mechanism of γ-secretase at molecular level is poorly understood.

Results: We found that the transmembrane domain (TMD) 1 of presenilin (PS) 1, a catalytic subunit for the γ-secretase, as a key modulatory domain for Aβ42 production. Aβ42-lowering and -raising γ-secretase modulators (GSMs) directly targeted TMD1 of PS1 and affected its structure. A point mutation in TMD1 caused an aberrant secretion of longer Aβ species including Aβ45 that are the precursor of Aβ42. We further found that the helical surface of TMD1 is involved in the binding of Aβ45/48 and that the binding was altered by GSMs as well as TMD1 mutation.

Conclusions: Binding between PS1 TMD1 and longer Aβ is critical for Aβ42 production.

Keywords: Presenilin, Secretases, Alzheimer disease, Intramembrane proteolysis, γ-Secretase modulator

Background

Several lines of evidence suggest that the accumulation of amyloid-β peptide (Aβ), a major component of senile plaques, is a common pathological feature in Alzheimer disease (AD) [1]. Aβ is generated through sequential cleavage by β- and γ-secretases of amyloid-β precursor protein (APP). γ-Secretase primarily cleaves APP to produce a C-terminal stub of APP (APP-CTF). Then, scission of APP-CTF by γ-secretase results in generation of various forms of Aβ with different C-terminal lengths. Especially, Aβ ending at the 42nd residue (Aβ42), the most aggregable species, is initially and predominantly deposited in AD brains [2]. Moreover, familial AD-linked mutations in *Psen* (*Presenilin; PS*) *1*, *Psen2* or *APP* genes cause an increase in Aβ42 generation. Thus, Aβ42 is considered as the most pathogenic species causative for AD [3].

γ-Secretase is an intramembrane-cleaving protease complex composed of four membrane spanning proteins: PS, Nicastrin, Aph-1 and Pen-2 [4,5]. Extensive biochemical studies showed that the γ-secretase-mediated intramembrane cleavage of APP occurs in a processive manner [6]; APP-CTF is primarily cleaved at the ε-site located around the membrane-cytoplasm boundary to produce Aβ49 or Aβ48. Subsequently, these longer Aβ peptides are processed by stepwise cleavages to secrete shorter Aβ in two predominant production lines: Aβ49 is processed to Aβ43/40 via Aβ46 (Aβ40 production line), and Aβ48 is processed to Aβ42/38 via Aβ45 (Aβ42 production line). PS forms a channel-like catalytic pore structure within the membrane, and is endoproteolyzed to generate N- and C-terminal fragments (NTF and CTF, respectively) during the assembly of the protease-active complex [7,8].

Recently, small compounds that selectively regulate Aβ42 production without affecting ε-cleavage emerged, which are termed γ-secretase modulators (GSMs) [9]. We have shown that a potent Aβ42-lowering compound, GSM-1, directly targets the PS1 TMD1 [10]. Moreover, using substituted cysteine accessibility method (SCAM), we identified two different regions within TMD1 of PS1, i.e., a hydrophobic luminal region and a hydrophilic portion facing the catalytic site [11], that are differently

* Correspondence: taisuke@mol.f.u-tokyo.ac.jp
[1]Department of Neuropathology and Neuroscience, Graduate School of Pharmaceutical Sciences, The University of Tokyo, 7-3-1 Hongo, Bunkyo-ku, Tokyo 113-0033, Japan
Full list of author information is available at the end of the article

involved in the action of GSM-1 [10]. However, the precise molecular mechanism whereby γ-secretase generates Aβ42, as well as the role of TMD1 in Aβ42 production, remains elusive. In this study, we identified TMD1 of PS1 as a regulatory domain for the processive cleavage of the Aβ42 production line.

Results

Fenofibrate directly targets the N-terminal fragment of presenilin 1

Fen-B [12] is a derivative of the Aβ42-raising GSM, fenofibrate [13], coupled to a biotin moiety. Previous report showed that Fen-B directly targeted APP-CTF by photo-crosslinking using recombinant proteins or microsomes under overexpression conditions. However, the possibility of a nonspecific binding of fenofibrate to high concentrations of APP in an artificial condition was not excluded [14,15]. We performed a photoaffinity labeling experiment with Fen-B using microsomes prepared from brains of wild-type mice. We found that endogenous PS1 NTF, but neither of other γ-secretase components (i.e., PS1 CTF, Nicastrin, Aph-1 and Pen-2) nor APP-CTF, was specifically precipitated (Figure 1A). In addition, we detected a biotinylated band of ~30 kDa, corresponding to the molecular weight of PS1 NTF, in the fraction incubated with Fen-B. To further confirm the specificity of labeling of PS1 NTF by Fen-B, membrane fractions of fibroblasts from *Psen1*$^{-/-}$/*Psen2*$^{-/-}$ double knockout mice (DKO) [16] with or without overexpression of His-tagged PS1 [17] were subjected to PAL. Biotinylated PS1 NTF was specifically precipitated, indicating that PS1 NTF is targeted by Fen-B (Figure 1B). Finally, a specific binding of Fen-B to SPP, another aspartic intramembranous cleaving protease, which shared homology with PS [18], was also observed (Figure 1C). Taken together, we concluded that the *bona fide* molecular target of fenofibrate, in the context of modulation of intramembrane cleavage, are PS1 and SPP, i.e., the enzyme moieties.

To narrow down the fenofibrate binding site within PS1 NTF, we employed the limited digestion approach by inserting a thrombin substrate sequence into PS1 [10]. γ-Secretase containing PS1-Th1 mutant, in which thrombin cleavable sequence was inserted between D110 and G111 in the hydrophilic loop 1, harbored γ-secretase activity and was sensitive to fenofibrate (Figure 2A). Eight kDa N-terminal fragment of PS1 NTF generated by thrombin cleavage of PS1-Th1 after Fen-B

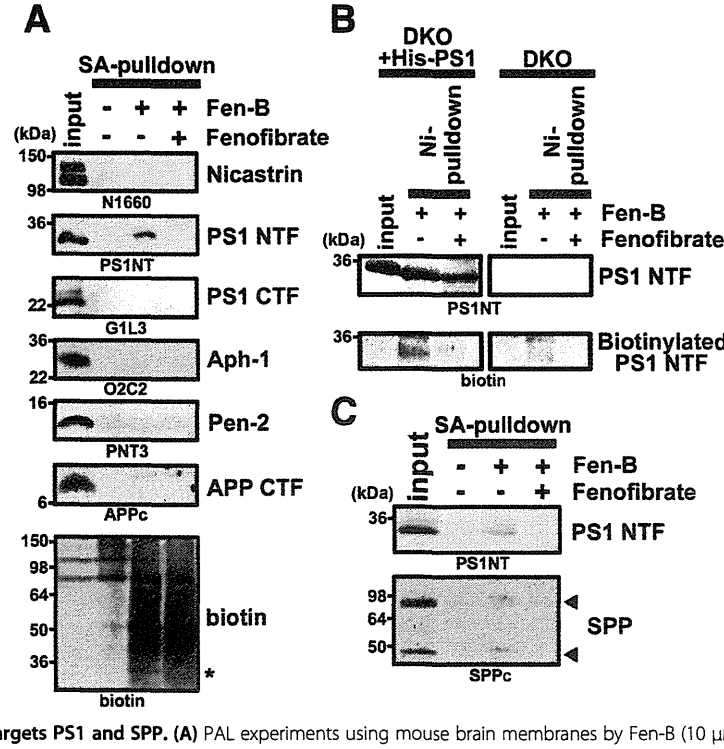

Figure 1 Fen-B directly targets PS1 and SPP. (A) PAL experiments using mouse brain membranes by Fen-B (10 μM). This labeling was competed by treatment with fenofibrate (200 μM). Note that only PS1 NTF was specifically labeled by Fen-B. Anti-biotin antibody also reacted with a band with ~30 kDa corresponding to PS1 NTF (an asterisk). **(B)** Fen-B labeling experiment for the DKO cells expressing His-tagged PS1. After PAL, His-tagged PS1 was purified with Ni^{2+}-affinity column and analyzed by immunoblotting. **(C)** Fen-B also bound endogenous monomeric as well as dimeric SPP (arrows) in CHO cell membranes.

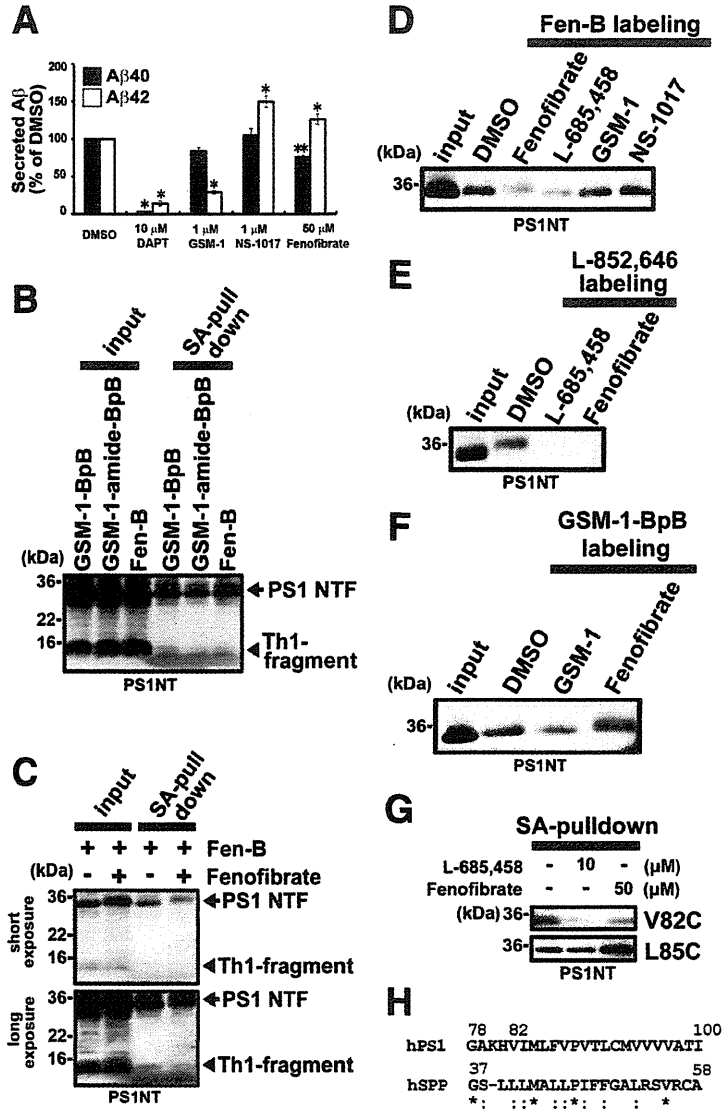

Figure 2 Cytosolic side of TMD1 forms a fenofibrate binding pocket. (A) Sensitivity of PS1-Th1 for GSMs. Effect of DAPT (10 μM), GSM-1 (1 μM), NS-1017 (1 μM) and fenofibrate (50 μM) on secreted Aβ from wild-type PS1 containing γ-secretase using DKO cells stably expressing APPNL (n = 3, mean ± SD, *p < 0.01, **p < 0.05 at Student's t test). **(B)** Thrombin digestion experiments were performed after PAL by GSM-1-BpB (1 μM), GSM-1-amide-BpB (1 μM) and Fen-B (10 μM). Note that cleaved Th1-fragment (arrowhead) was precipitated and detected by anti-PS1 NTF antibody. **(C)** Labeling competition analysis of Fen-B (10 μM) in the presence of fenofibrate (100 μM) using PS1-Th1 microsomes. Upper and lower panels show short and long exposures, respectively. **(D)** Labeling competition analyses were performed with fenofibrate (100 μM), L-685,458 (10 μM), GSM-1 (100 μM) and NS-1017 (100 μM) for the labeling of PS1 NTF by Fen-B (10 μM). **(E)** Labeling competition experiment with L-685,458 (10 μM) and fenofibrate (100 μM) for the labeling of PS1 NTF by L-852,646 (100 nM). **(F)** Labeling competition analysis by GSM-1-BpB (1 μM) in the presence of GSM-1 (100 μM) or fenofibrate (100 μM) using CHO cell microsomes. **(G)** SCAM analyses of microsomes from DKO cells expressing single-Cys mt PS1 containing one Cys at 82 or 85 positions in the presence or absence of indicated compounds. Note that the labeling of V82C was decreased and of L85C was increased by preincubation with fenofibrate. **(H)** Alignment of amino acid residues of PS1 TMD1 (78th to 100th residues) and 37th to 58th residues of SPP, which includes predicted TMD1 (32nd to 54th residues [19]). Asterisks and colons indicate conserved and similar amino acids, respectively.

crosslinking was specifically precipitated in a similar fashion to that by phenylpiperidine-type photoprobes, suggesting that Fen-B also targets to the most N-terminal region of PS1, including TMD1 (Figure 2B and C). We showed that the cytosolic side of TMD1 participates in the catalytic hydrophilic pore [7,11]. To analyze the relationship between the fenofibrate binding site and the catalytic site within TMD1, we employed the cross-

competition analysis in Fen-B labeling using different classes of compounds. Labeling of PS1 NTF by Fen-B was diminished by L-685,458, that directly targets the cytosolic side of TMD1 (Figure 2D) [11]. Consistent with this, labeling of PS1 NTF by L-852,646, an L-685,458-based photoprobe, was inhibited by fenofibrate (Figure 2E). In contrast, neither GSM-1 nor NS-1017, which targets the luminal region of TMD1, affected the binding of Fen-B (Figure 2D). Moreover, biotinylation of PS1 NTF by GSM-1-BpB was hardly affected by fenofibrate (Figure 2F), suggesting that the binding site of fenofibrate is distinct from that of GSM-1 within TMD1. We then performed a labeling competition experiment in SCAM [7,11], the latter being a biochemical method to deduce the structure of the membrane protein by position-specific biotinylation and to identify the targeting site of the compound of interest. Preincubation of fenofibrate decreased the biotinylation at Val82, supporting the notion that fenofibrate targets the catalytic site. In contrast, labeling of Leu85 was increased, indicating that fenofibrate evokes a conformational change of the catalytic site in TMD1 (Figure 2G). Intriguingly, Gly37 to Ala58 of SPP, which encompassed the predicted SPP TMD1 (Ile32 to Ser54) [19], showed a substantial homology to primary sequence of N-terminal region of PS1 TMD1 (i.e., Gly78 to Ile100) (Figure 2H), suggesting the possibility that fenofibrate targets to the predicted SPP TMD1. Taken together with the results of chemical biological experiments, the binding site of fenofibrate was estimated to locate around Val82 in TMD1, leading to the conformational change of the catalytic site of γ-secretase.

Intermediate longer A was secreted by TMD1 mutant PS1

This finding prompted us to hypothesize that TMD1 is potentially involved in the regulation of the processivity of γ-secretase to generate Aβ42. To address this issue, we screened single cysteine (single-Cys) mutants of TMD1 in cysteine-less PS1 used in SCAM. While cysteine-less PS1 increased Aβ42(43)/Aβ40 ratio compared to that of wild-type PS1-expressing cells, some single-Cys mutants showed further augmentation in Aβ42(43)/Aβ40 ratio (Figure 3A). Among these mutants, P88C mutant showed a dramatic increase in the Aβ42 (43)/Aβ40 ratio. To further analyze the functional significance of Pro88 in the processive cleavage, we analyzed two PS1 mutants, P88C and P88L. Surprisingly, P88L mutation caused an increase in the Aβ42(43)/Aβ40 ratio, to a level higher than that with L166P mutant PS1 (Figure 3C and D), one of the most potent pathogenic PS1 mutations [20]. In addition, P88L mutant elicited secretion of the intermediate, longer form of Aβ, i.e. Aβ45

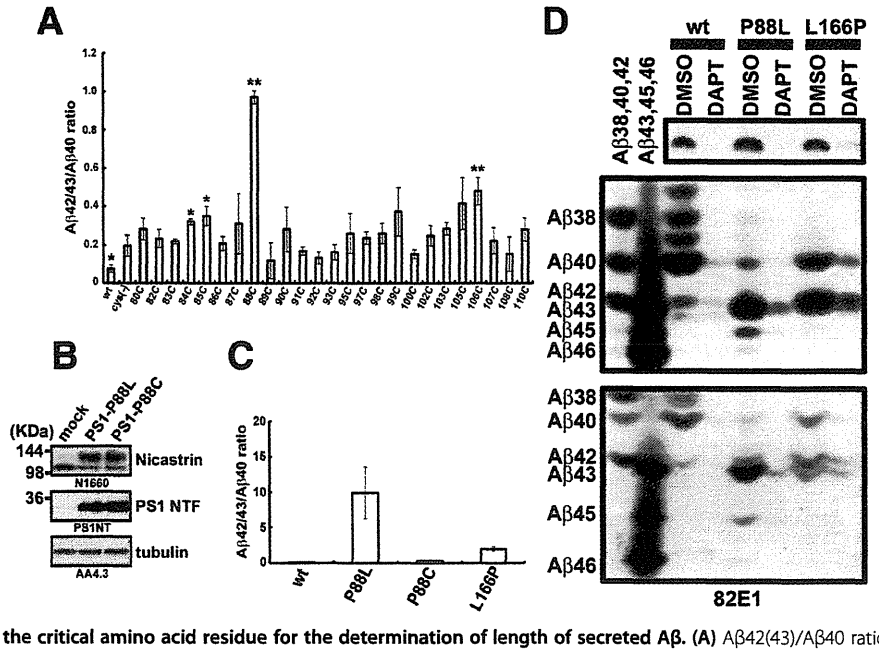

Figure 3 Pro88 is the critical amino acid residue for the determination of length of secreted Aβ. (A) Aβ42(43)/Aβ40 ratio in secreted Aβ from DKO cells expressing Single-Cys mt PS1. Conditioned media were analyzed by ELISA (n = 3, mean ± SD, *p < 0.05, **p < 0.01 (Compared with Cys-less) at Student's t test). **(B)** Immunoblotting analysis of DKO cell lysate expressing PS1 mutant carrying P88C or P88L by indicated antibodies. **(C)** Aβ42(43)/Aβ40 ratio in secreted Aβ from DKO cells in **(B)** measured by ELISA (n = 3, mean ± SD). **(D)** Urea-SDS gel analysis for secreted Aβ from DKO cells expressing wild-type PS1, PS1 with P88L or PS1 with L166P mutation. Conditioned media of cells treated with 10 μM DAPT were also analyzed. Two types of Urea-SDS gels were used to obtain better resolution in the detection of longer Aβ peptides (i.e., Aβ45 and Aβ46).

and Aβ46, but neither in the wild-type nor L166P mutant PS1 (Figure 3D). These data strongly implicated TMD1 in the regulation of the C-terminal length of Aβ.

GSMs and P88L mutation affected the interaction between TMD1 and longer Aβ species

Our unexpected observation of an abnormal secretion of longer Aβ45 from cells expressing P88L mutant PS1 prompted us to further investigate the functional role of TMD1 during the enzymatic process, especially the processive cleavage. Notably, previous reports indicated that a region between Val82 to Ser132 encompassing TMD1 directly participates in the interaction with γ-secretase substrates (i.e., APP-CTF) *in vitro* [21-23]. Moreover, Aβ46 has been shown to accumulate by DAPT, which inhibits processive cleavage, and to be coimmunoprecipitated with PS1 [23,24]. These results implied the possibility that TMD1 directly recognizes the longer Aβ species during the processive cleavage of γ-secretase. To test this idea, we performed *in vitro* binding assays of various longer Aβ species with purified GST, GST-PS1$_{1\text{-}110}$ and GST-TM1mt$_{1\text{-}110}$, the latter harboring the TMD1 sequence (i.e., Val82 to Ile100) replaced with a TMD of an unrelated membrane protein, CLAC-P [10,25] (Figure 4A and B). Replacement of TMD1 of PS1 with CLAC-P sequence abolished the γ-secretase activity [17] as well as binding of GSM-1-BpB *in vitro* [10] (Figure 4C), indicating chimeric PS1 with CLAC sequence has a distinct property. Then synthetic Aβ peptides were coincubated with recombinant proteins and pulled down by glutathione sepharose (Figure 4D). In this condition, we detected specific binding of recombinant C99-FLAG to GST-PS1$_{1\text{-}110}$, as previously reported by Annaert et al [21]. In addition, we detected binding of all synthetic longer Aβ peptides (Aβ49, Aβ48, Aβ46, Aβ45, Aβ43) with GST-PS1$_{1\text{-}110}$, suggesting that TMD1 of PS1 directly binds to longer Aβ peptides, and that the cytoplasmic domain of APP is not involved in this binding. Unexpectedly, GST-TM1mt$_{1\text{-}110}$ was capable of interacting with C99-FLAG as well as with peptides belonging to the Aβ40 production line (Aβ49, Aβ46 and Aβ43). However, the binding of Aβ species of the Aβ42 production line (i.e., Aβ48 and Aβ45) was significantly reduced by swapping the TMD1 sequence (Figure 4D). We further analyzed the effect of TMD1-targeting GSMs as well as P88L mutation on the binding of Aβ45 and Aβ48 to TMD1. Intriguingly, GSM-1 augmented the interaction of TMD1 with Aβ45 as well as Aβ48, whereas it was reduced by fenofibrate (Figure 4E). In addition, introduction of P88L mutation in GST PS1-$_{1\text{-}110}$ decreased the pull down of Aβ45 (Figure 4F). Finally, we observed a specific binding of Aβ48 with native PS1

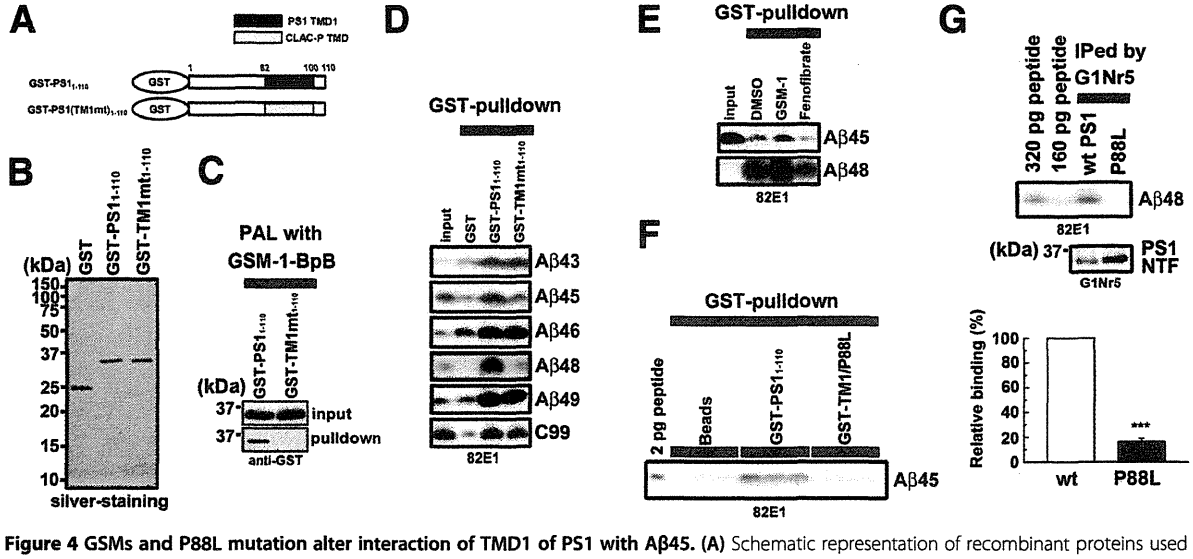

Figure 4 GSMs and P88L mutation alter interaction of TMD1 of PS1 with Aβ45. (A) Schematic representation of recombinant proteins used in this study. **(B)** GST and GST-fused recombinant proteins were purified by glutathione sepharose and/or Mono Q column. The purity of purified recombinant proteins was confirmed by silver staining. **(C)** GSM-1-BpB (4 nM) labeling experiment for GST-PS1$_{1\text{-}110}$ and TMD1 swapping mutant, GST-TM1mt$_{1\text{-}110}$ (0.19 μg). Samples were preincubated with photoprobes on ice for 10 min, and then irradiated for 60 min. **(D)** Pull down assay of GST-fused recombinant proteins mixed with longer Aβ (Aβ43/45/46/48/49) (1 nM). After incubation with glutathione sepharose, all samples were washed and subjected to immunoblot. **(E)** The effects of GSM-1 (25 μM) or fenofibrate (100 μM) on the interaction of GST-PS1$_{1\text{-}110}$ with longer Aβ peptides. Recombinant proteins were preincubated with GSMs and then incubated with longer Aβ peptides. Protein complexes were pulled down by glutathione sepharose and analyzed by immunoblot. **(F)** The effect of P88L mutation on the binding of Aβ45 peptide to GST-PS1$_{1\text{-}110}$. **(G)** Binding of Aβ48 peptide to native PS1 protein expressed in mammalian cells. Densitometric analysis of relative levels of the bound Aβ48 was shown at the below (n = 3, mean ± SD, ***p <0.001 at Student's t test).

protein expressed in the mammalian cells, and this interaction was almost diminished by the P88L mutation (Figure 4G). We did not observe specific binding of Aβ45 with PS1 holoprotein expressed in mammalian cells, presumably due to weak binding of Aβ45 to PS1 protein. Nevertheless, these data suggest that the processivity of the γ-secretase for Aβ42 production is defined by the tenacity of interaction between TMD1 and longer Aβ, which may determine the retention of the substrate in the catalytic site. Collectively, we uncovered the significant function of TMD1 of PS1 as a binding site for the longer Aβ species, especially Aβ45 and Aβ48, during the processive cleavage of the Aβ42 production line, and the effects of GSMs on Aβ42 production by changing the affinity between TMD1 and the longer Aβ peptides.

Discussion

Understanding the molecular mechanism of the processive cleavage by γ-secretase is critical to the development of effective GSMs. We previously reported that phenylpiperidine-type GSMs are bound to TMD1 of PS1 [10]. Here, we further showed that fenofibrate, an Aβ42-raising GSM, also directly targets TMD1, while Fen-B was reported as APP-targeting photoprobe [12]. Recently, some papers reported that large amount of Aβ42 or C99 forms aggregates that cause non-specific binding to GSMs [14,15]. Therefore, we have used brain microsomes obtained from wild-type mouse for the photocrosslinking experiment.

Scissile bonds for processive cleavage by γ-secretase have hypothetically been mapped on different surfaces in the α-helical model of APP TMD [26]. This raises the possibility that the distinct processive cleavages by γ-secretase, i.e., those leading to production of Aβ49-46-43-40 or Aβ48-45-42-38, are determined by the recognition of one or the other of the specific helical surfaces. However, the domain on γ-secretase that recognizes the helical surface on the substrate is yet to be identified. It has previously been suggested that TMD1 of PS1 is involved in the binding of APP-CTF, a direct substrate of γ-secretase [21,22]. Here we found that longer Aβ peptides that are generated as intermediate products in the Aβ42 production line (i.e., Aβ45 and Aβ48), which also are direct substrates for the processive cleavage, retain the capacity to interact with TMD1 of PS1. It is highly likely that the "gripping tenacity" of the substrate binding site facing the catalytic pore would determine the processivity of Aβ48 and Aβ45 on the Aβ42 production line, which can be modulated by small compounds. Consistently, Okochi et al. have recently reported that Aβ42 is bound to the γ-secretase complex [27] and the binding was modulated by GSMs, although they have not identified the binding site of Aβ within the enzyme complex. Thus, we propose that TMD1 of PS1 functions as a binding site of longer Aβ species for γ-secretase during the processive cleavage, which specifically determines the efficiency of the processive cleavage of the Aβ42 production line. Structural analyses suggested that the catalytic cavities of rhomboid protease [28], another intramembrane-cleaving enzyme, or those of FlaK [29] and PSH [30], archaeal GxGD proteases, are unable to accommodate all the amino acid residues of the transmembrane sequence of the substrates. This suggests that a major part of the TMD of substrates remains within the membrane and is gripped by enzymes to incorporate the cleavage site into the intramembrane catalytic site during proteolysis. While the precise structure of human PS1 still remains unclear, our SCAM results on PS1 [11], as well as the recently reported x-ray crystal structure of PSH [30], the latter being composed of 9-transmembrane domains similarly to human PS1, altogether suggested that TMD1 locates in proximity to the catalytic aspartate in TMD7. The results of these structural analyses also support our notion that TMD1 functions as a substrate binding domain during the processive cleavage by γ-secretase.

TMD1 of PS1 bound not only to longer Aβ peptides of the Aβ42 production line, but to those of Aβ40 line (Figure 4D). P88L mutation in TMD1 of PS1 caused an increased secretion of not only Aβ45, but also Aβ43 and Aβ46 (Figure 3F), suggesting that the interaction between TMD1 and longer Aβ species is also critical for the processivity in the Aβ40 production line. Intriguingly, swapping TMD1 sequence of PS1 with that of CLAC-P, an unrelated membrane protein, did not affect the binding of Aβ43, Aβ46 and Aβ49 peptides. In the helical net diagram, similar side chains at the luminal side of PS1 TMD1 and CLAC-P TMD comprised an interface on the α-helical model only in one side (Figure 5A and B) [31]. Thus, one helical surface of TMD1 is involved in the binding of longer Aβ species in the Aβ40 production line, whereas the other surface specifically interacts with those in the Aβ42 production line in the PSH-based PS1 model (Figure 5C). Pharmacological and chemical biological studies suggest that the substrate enters the catalytic site via the initial substrate binding site, in which TMD2, 6 and 9 are involved [17]. Especially, TMD6 and 9 have been implicated in the lateral entry of the substrate from the crystal structure of PSH [30]. However, helical peptide-type GSIs that target the initial substrate binding site equally inhibited the production of Aβ40 or Aβ42 [32,33]. Thus, we hypothesize that C99 or longer Aβ is gripped by TMD1 after the lateral entry (Figure 5D). Structural model also suggested that residues related to the Aβ42 production line in the luminal side of TMD1 are located on the surface of PS1 polypeptide, which might be targeted by GSM-1 [10]. In fact, several side chain interactions have been identified in

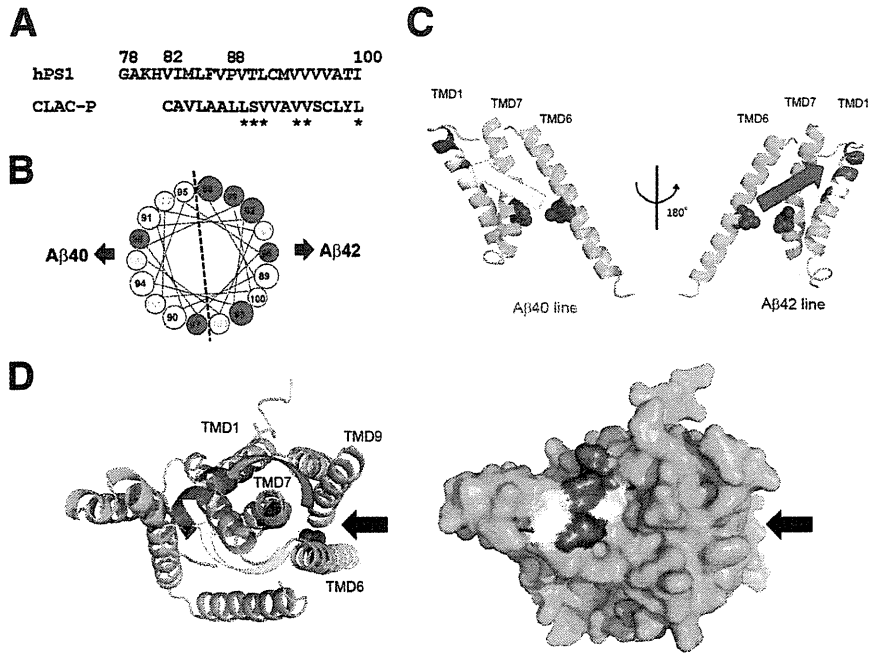

Figure 5 Hypothetical model of the role of PS1 TMD1 in Aβ42 generation. (A and B) Alignment of amino acid residues of the human PS1 TMD1 and CLAC-P. In the swap mutant PS1, 82nd to 100th residues were replaced with CLAC-P TMD. Residues with similar side chains are labeled with asterisks in **(A)** and as yellow circles in **(B). (C)** Modified structural model of PS1 based on PSH structure kindly provided from Dr. Y. Shi [30]. Side views of the ribbon model of TMD1, 6 and 7 generated by Pymol are shown. Yellow and purple residues correspond to those in **(B)**. Possible approaches to the catalytic aspartates (red spheres) for Aβ40 and Aβ42 production lines are shown by yellow and purple arrows, respectively. TMD1 grips the substrate to prevent its liberation during the processive cleavage. Helix-helix interaction of longer Aβ with TMD1 determines the major production line (i.e., Aβ40 or Aβ42) of processive cleavage. **(D)** Top views of the whole PS1 model (left; ribbon diagram; right, surface model) generated by Pymol are shown. Putative substrate entry site [30] is shown as black arrows.

TMD1 and the neighboring TMDs [30]. However, we have previously suggested a piston-like vertical movement of TMD1 by SCAM [34], supporting our view that dynamic conformational changes would take place during the catalytic reaction. Intriguingly, the reason why the efficiency of Aβ42 production is always lower than that of Aβ40 in any cell types [35] has been unknown. Considering the positions of the first ε-cleavage sites located on the opposite sides of the helical surfaces predicted for the Aβ40 and Aβ42 production lines, it is tempting to speculate that an approach of the substrate from an unfavored direction (pink arrow, Figure 5) to the catalytic site in terms of stereochemistry might explain the lower efficiency of cleavage in the Aβ42 production line (Figure 5C and D). However, the other TMDs might be also involved in the recognition of Aβ42, and GSMs could allosterically affect these other regions including initial substrate binding site in PS1. Biochemical analysis to identify the other binding domain for longer Aβ peptides belonging to the Aβ40 production line would provide further molecular insights regarding the mechanism of action of GSMs. Also structural analysis of mammalian PS1 carrying P88L mutation might unveil further mechanistic role of TMD1 in the trimming process by γ-secretase. In sum, we revealed that TMD1, a previously identified target region of GSMs, participates in the Aβ42 generation as a binding site that docks longer Aβ species as intermediate substrates for γ-secretase. Our observations may shed light on the molecular mechanism of the processive cleavage by γ-secretase, contributing to the development of potent and selective Aβ42-lowering compounds for AD.

Conclusions

Fenofibrate directly bound to TMD1 of PS1 to induce the conformational changes in the catalytic site of the γ-secretase. P88L mutation in TMD1 caused an aberrant secretion of longer Aβ polypeptides (i.e., Aβ45 or Aβ46), indicating that TMD1 is involved in the regulation of C-terminal length of Aβ. Finally, we found that TMD1 contains a binding site for the longer Aβ species, and GSMs affect Aβ42 production by changing the affinity between TMD1 and longer Aβ. Our results suggest that TMD1 functions as a substrate binding domain during the processive cleavage by γ-secretase.